PERGAMON

International Journal of Solids and Structures 39 (2002) 3131–3158

INTERNATIONAL JOURNAL OF SOLIDS and STRUCTURES

www.elsevier.com/locate/ijsolstr

Decoupled formulation of piezoelectric elasticity under generalized plane deformation and its application to wedge problems

Ching-Hwei Chue *, Chung-De Chen

Department of Mechanical Engineering, National Cheng Kung University, 70101 Tainan, Taiwan, ROC

Received 28 July 2001; received in revised form 1 March 2002

Abstract

This paper presents the formulation of piezoelectric elasticity under generalized plane deformation derived from the three-dimensional theory. There are four decoupled classes in the generalized plane deformation formulation, i.e. when $l_3(\mu) = l_2^*(\mu) = 0$, $l_3(\mu) = l_3^*(\mu) = 0$, $l_3^*(\mu) = l_2^*(\mu) = 0$ or $l_3(\mu) = l_3^*(\mu) = l_2^*(\mu) = 0$. Only the inplane fields of the first class and the antiplane field of the second class include the piezoelectric effect. Several examples of wedge problem often encountered in smart structures, such as sensors or actuators are studied to examine the stress singularity near the apex of the structure. The bonded materials to the PZT-4 wedge are PZT-5, graphite/epoxy or aluminum (conductor). The influencing factors on the singular behavior of the electro-elastic fields include the wedge angle, material type, poling direction, and the boundary and interface conditions. The numerical results of the first case are compared with Xu's graphs and some comments are made in detail. In addition, some new results regarding the antiplane stress singularity of the second class are obtained via the case study. The coupled singularity solutions under generalized plane deformation are also investigated to seek the conditions of the weakest or vanishing singular stress fields.

Keywords: Piezoelectric; Stress singularity; Lekhnitskii; Wedge structures

1. Introduction

Piezoelectric materials are widely used in actuators due to its electro-mechanical coupling behavior (Gandhi and Thompson, 1992; Uchino, 1997). The actuators involving piezoelectric materials are usually synthesized with fiber reinforced composites, electrodes, and other piezoelectric materials. The local regions of the bonded materials are considered as wedges as shown in Fig. 1. Due to the geometric and material discontinuities, the stresses approach to infinity theoretically at the apex of the wedge, i.e., the stresses are singular. The failures initiate from the apex of the wedges frequently if the devices are operated in severe environments or under strenuous loading conditions.

* Corresponding author. Tel.: +886-6-2757575x62165; fax: +886-6-2352973.
E-mail address: chchue@mail.ncku.edu.tw (C.-H. Chue).

0020-7683/02/$ - see front matter
PII: S0020-7683(02)00247-0

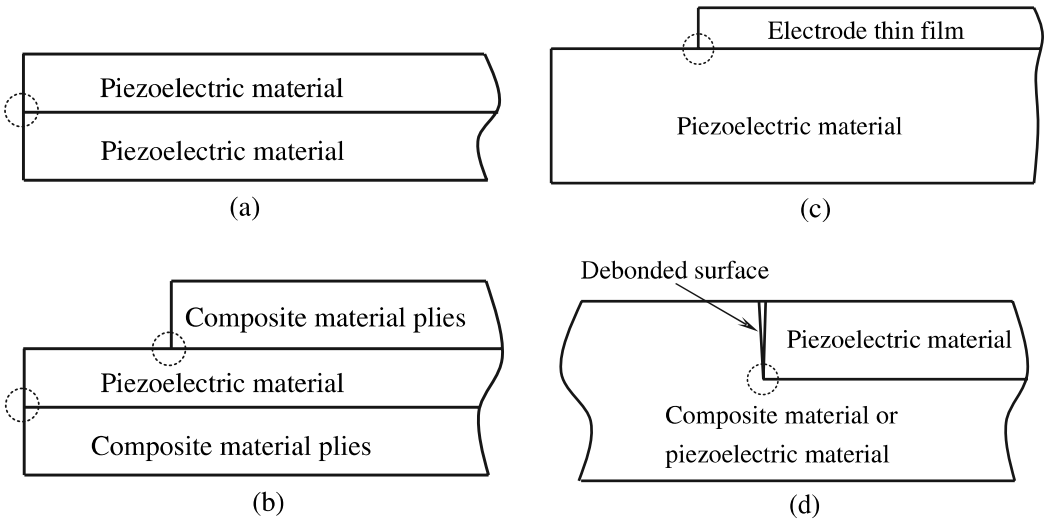

Fig. 1. Several typical wedge structures in actuators: (a) Piezoelectric–piezoelectric wedges; (b) piezoelectric–composite wedges; (c) piezoelectric–conductor wedges; and (d) debonded junctions involving piezoelectric materials.

Several different approaches to electro-elastic field have been proposed. Barnett and Lothe (1975) extended Stroh's six-dimensional framework (Stroh, 1962) to an eight-dimensional formalism to solve a generalized plane problem of piezoelectric body. Sosa (1991) extended the ideas developed by Lekhnitskii (1963) in anisotropic elasticity to obtain the plane strain formulation of the piezoelectric problems. In Sosa's study, a six-order differential operator was performed and was used to solve the inplane problem in piezoelectric media with defects. Chen and Lai (1997) and Chen and Yen (1998) used the generalized Lekhnitskii's formulation to formulate piezoelectric medium under generalized plane deformation.

The fracture mechanics have been widely investigated in the past few years. Parton (1976) first studied the fracture problem in piezoelectric materials from a theoretical stand point of view. Sosa and Pak (1990) used eigenfunction expansion to solve the stress and electric fields of a crack in a piezoelectric material. The results show the characteristic $r^{-0.5}$ singular behavior of the stress tensor in the vicinity of the crack. Kuo and Barnett (1991) studied the crack and interface crack in piezoelectric mediums by using an extended Stroh formulation. The results showed that the singularity orders of interface crack may not be -0.5. In addition, Shindo et al. (1996, 1997) and Narita and Shindo (1998, 1999) studied the antiplane shear crack problems in a piezoelectric medium as well as interface cracking between piezoelectric and orthotropic layers.

Although the crack problems of piezoelectric materials have been widely investigated in the past decade, the wedge problems involving piezoelectric materials, composite materials, and conductors are rarely reported in the literature. To the author's knowledge, there is only one paper discussing the piezoelectric wedges (Xu and Rajapakse, 2000). Before this, the isotropic and/or anisotropic wedge and junction problems had been extensively studied (e.g. Tranter, 1948; Williams, 1952; Bogy, 1971; Theocaris, 1974; Bogy, 1972; Delale, 1984; Ting, 1986; Ma and Hour, 1989; Huang and Chen, 1994; Chen, 1998).

The polarized piezoelectric material possesses some symmetry for certain poling orientations. In Xu's paper, the poling axis is oriented in the x–y plane, which thereby limits the investigation of the piezoelectric effect to the inplane field. If the poling direction is along the z-axis, the piezoelectric wedge problem will be decoupled into inplane and antiplane problems. The inplane field simply consists of the elastic deformation of stresses $(\sigma_x, \sigma_y, \tau_{xy})$ and displacements (u, v). The antiplane field couples the antiplane elastic deformation

$(\tau_{xz}, \tau_{yz}, w)$ with the inplane electric parameters $(D_x, D_y, E_x, E_y, \Phi)$. Based on the fundamental study of the coupling behavior by using the eigenfunction expansion, the singularity stress behavior of piezoelectric wedge problems is investigated in this paper.

2. Basic formulation

The constitutive equation of piezoelectric materials is given as follows:

$$\begin{Bmatrix} \varepsilon_x \\ \varepsilon_y \\ \varepsilon_z \\ \gamma_{yz} \\ \gamma_{xz} \\ \gamma_{xy} \\ -E_x \\ -E_y \\ -E_z \end{Bmatrix} = \begin{bmatrix} s_{11} & s_{12} & s_{13} & s_{14} & s_{15} & s_{16} & g_{11} & g_{21} & g_{31} \\ s_{12} & s_{22} & s_{23} & s_{24} & s_{25} & s_{26} & g_{12} & g_{22} & g_{32} \\ s_{13} & s_{23} & s_{33} & s_{34} & s_{35} & s_{36} & g_{13} & g_{23} & g_{33} \\ s_{14} & s_{24} & s_{34} & s_{44} & s_{45} & s_{46} & g_{14} & g_{24} & g_{34} \\ s_{15} & s_{25} & s_{35} & s_{45} & s_{55} & s_{56} & g_{15} & g_{25} & g_{35} \\ s_{16} & s_{26} & s_{36} & s_{46} & s_{56} & s_{66} & g_{16} & g_{26} & g_{36} \\ g_{11} & g_{12} & g_{13} & g_{14} & g_{15} & g_{16} & -\beta_{11} & -\beta_{12} & -\beta_{13} \\ g_{21} & g_{22} & g_{23} & g_{24} & g_{25} & g_{26} & -\beta_{12} & -\beta_{22} & -\beta_{23} \\ g_{31} & g_{32} & g_{33} & g_{34} & g_{35} & g_{36} & -\beta_{13} & -\beta_{23} & -\beta_{33} \end{bmatrix} \begin{Bmatrix} \sigma_x \\ \sigma_y \\ \sigma_z \\ \tau_{yz} \\ \tau_{xz} \\ \tau_{xy} \\ D_x \\ D_y \\ D_z \end{Bmatrix} \tag{1}$$

where ε_i, γ_{ij} are normal and shear strains, E_i are electric fields, σ_i, τ_{ij} are normal and shear stresses, D_i are electric displacements, s_{ij} are compliance constants, g_{ij} are piezoelectric constants, and β_{ij} are impermittivities. Consider a homogeneous piezoelectric body (material 1) bonded by another homogeneous body (material 2) shown in Fig. 2. The length in longitudinal direction is assumed to be infinite. The body is referred to the Cartesian coordinates x, y, z. The z-axis is parallel to the longitudinal direction. The body is assumed to be generalized plane deformation and subjected to generalized plane electric field. All physical quantities, such as stresses, strains, displacements, electric fields, electric displacements and electric potentials, are functions of x and y only. Eq. (1) can be reduced to the following equation (see Appendix A for details)

$$\begin{Bmatrix} \partial u/\partial x \\ \partial v/\partial y \\ \partial w/\partial y \\ \partial w/\partial x \\ \partial u/\partial y + \partial v/\partial x \\ \partial \Phi/\partial x \\ \partial \Phi/\partial y \end{Bmatrix} = \begin{bmatrix} a_{11} & a_{12} & a_{14} & a_{15} & a_{16} & b_{11} & b_{21} \\ a_{12} & a_{22} & a_{24} & a_{25} & a_{26} & b_{12} & b_{22} \\ a_{14} & a_{24} & a_{44} & a_{45} & a_{46} & b_{14} & b_{24} \\ a_{15} & a_{25} & a_{45} & a_{55} & a_{56} & b_{15} & b_{25} \\ a_{16} & a_{26} & a_{46} & a_{56} & a_{66} & b_{16} & b_{26} \\ b_{11} & b_{12} & b_{14} & b_{15} & b_{16} & -d_{11} & -d_{12} \\ b_{21} & b_{22} & b_{24} & b_{25} & b_{26} & -d_{12} & -d_{22} \end{bmatrix} \begin{Bmatrix} \sigma_x \\ \sigma_y \\ \tau_{yz} \\ \tau_{xz} \\ \tau_{xy} \\ D_x \\ D_y \end{Bmatrix} \tag{2}$$

where u, v, w, and Φ denote the displacements in the x-, y-, z-direction and electric potential, respectively. a_{ij}, b_{ij}, d_{ij} are the reduced material constants defined as

$$a_{ij} = s_{ij} - \frac{s_{i3}s_{j3}}{s_{33}} + \frac{(g_{3i} - s_{i3}g_{33}/s_{33})(g_{3j} - s_{j3}g_{33}/s_{33})}{\beta_{33} + g_{33}g_{33}/s_{33}} \quad i,j = 1,\ldots,6 \tag{3a}$$

$$b_{ij} = g_{ij} - \frac{s_{j3}g_{i3}}{s_{33}} - \frac{(\beta_{i3} + g_{i3}g_{33}/s_{33})(g_{3j} - s_{j3}g_{33}/s_{33})}{\beta_{33} + g_{33}g_{33}/s_{33}} \quad i = 1,2,\ \ j = 1,\ldots,6 \tag{3b}$$

$$d_{ij} = \beta_{ij} + \frac{g_{i3}g_{j3}}{s_{33}} - \frac{(\beta_{i3} + g_{i3}g_{33}/s_{33})(\beta_{j3} + g_{j3}g_{33}/s_{33})}{\beta_{33} + g_{33}g_{33}/s_{33}} \quad i,j = 1,2 \tag{3c}$$

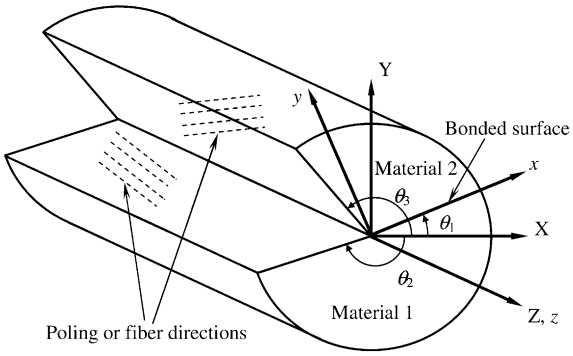

Fig. 2. The bimaterial wedge.

In the absence of body force and free charge, define the stress functions F, Ψ and the electric displacement function ϕ as follows

$$\sigma_x = \frac{\partial^2 F}{\partial y^2}, \quad \sigma_y = \frac{\partial^2 F}{\partial x^2}, \quad \tau_{xy} = -\frac{\partial^2 F}{\partial x \partial y}, \quad \tau_{xz} = \frac{\partial \Psi}{\partial y}, \quad \tau_{xz} = -\frac{\partial \Psi}{\partial x}, \quad D_x = \frac{\partial \phi}{\partial y}, \quad D_y = -\frac{\partial \phi}{\partial x} \tag{4}$$

It can be shown that F, Ψ and ϕ satisfy the equilibrium and Maxwell's equation automatically. Eliminating u, v, w, and Φ by differentiating (i.e., compatibility equations for strain and electrical fields), it gives

$$L_4 F + L_3 \Psi + L_3^* \phi = 0 \tag{5a}$$

$$L_3 F + L_2 \Psi + L_2^* \phi = 0 \tag{5b}$$

$$L_3^* F + L_2^* \Psi + L_2^{**} \phi = 0 \tag{5c}$$

where

$$L_4 = a_{22}\frac{\partial^4}{\partial x^4} - 2a_{26}\frac{\partial^4}{\partial x^3 \partial y} + (2a_{12} + a_{66})\frac{\partial^4}{\partial x^2 \partial y^2} - 2a_{16}\frac{\partial^4}{\partial x \partial y^3} + a_{11}\frac{\partial^4}{\partial y^4} \tag{6a}$$

$$L_3 = -a_{24}\frac{\partial^3}{\partial x^3} + (a_{25} + a_{46})\frac{\partial^3}{\partial x^2 \partial y} - (a_{14} + a_{56})\frac{\partial^3}{\partial x \partial y^2} + a_{15}\frac{\partial^3}{\partial y^3} \tag{6b}$$

$$L_3^* = -b_{22}\frac{\partial^3}{\partial x^3} + (b_{12} + b_{26})\frac{\partial^3}{\partial x^2 \partial y} - (b_{21} + b_{16})\frac{\partial^3}{\partial x \partial y^2} + b_{11}\frac{\partial^3}{\partial y^3} \tag{6c}$$

$$L_2 = a_{44}\frac{\partial^2}{\partial x^2} - 2a_{45}\frac{\partial^2}{\partial x \partial y} + a_{55}\frac{\partial^2}{\partial y^2} \tag{6d}$$

$$L_2^* = b_{24}\frac{\partial^2}{\partial x^2} - (b_{14} + b_{25})\frac{\partial^2}{\partial x \partial y} + b_{15}\frac{\partial^2}{\partial y^2} \tag{6e}$$

$$L_2^{**} = -d_{22}\frac{\partial^2}{\partial x^2} + 2d_{12}\frac{\partial^2}{\partial x \partial y} - d_{11}\frac{\partial^2}{\partial y^2} \tag{6f}$$

Eliminating Ψ and ϕ in Eqs. (5a)–(5c) yields

$$L_8 F = 0 \tag{7}$$

where

$$L_8 = L_4 L_2 L_2^{**} + 2L_3 L_3^* L_2^* - L_3^* L_3^* L_2 - L_4 L_2^* L_2^* - L_3 L_3 L_2^{**} \tag{8}$$

Set $F = F(x + \mu y)$ and μ is a complex number. Therefore the characteristic equation of Eq. (7) is

$$l_8(\mu) = l_4(\mu) l_2(\mu) l_2^{**}(\mu) + 2l_3(\mu) l_3^*(\mu) l_2^*(\mu) - l_3^*(\mu) l_3^*(\mu) l_2(\mu) - l_4(\mu) l_2^*(\mu) l_2^*(\mu) - l_3(\mu) l_3(\mu) l_2^{**}(\mu) = 0 \tag{9}$$

where

$$l_4(\mu) = a_{11}\mu^4 - 2a_{16}\mu^3 + (2a_{12} + a_{66})\mu^2 - 2a_{26}\mu + a_{22} \tag{10a}$$

$$l_3(\mu) = a_{15}\mu^3 - (a_{14} + a_{56})\mu^2 + (a_{25} + a_{46})\mu - a_{24} \tag{10b}$$

$$l_3^*(\mu) = b_{11}\mu^3 - (b_{21} + b_{16})\mu^2 + (b_{12} + b_{26})\mu - b_{22} \tag{10c}$$

$$l_2(\mu) = a_{55}\mu^2 - 2a_{45}\mu + a_{44} \tag{10d}$$

$$l_2^*(\mu) = b_{15}\mu^2 - (b_{14} + b_{25})\mu + b_{24} \tag{10e}$$

$$l_2^{**}(\mu) = -d_{11}\mu^2 + 2d_{12}\mu - d_{22} \tag{10f}$$

It can be shown that the roots of Eq. (9), denoted as μ_k $(k = 1, 2, \ldots, 8)$, are complex numbers (Suo et al., 1992). For convenience, the imaginary parts of μ_1, μ_2, μ_3 and μ_4 are chosen to be positive. μ_5, μ_6, μ_7 and μ_8 are conjugate of μ_1, μ_2, μ_3 and μ_4, respectively. The solution of Eqs. (5a)–(5c) can be written as

$$F = \mathrm{Re}\left[\sum_{k=1}^{4} F_k(x + \mu_k y)\right] \tag{11a}$$

Similarly,

$$\Psi = \mathrm{Re}\left[\sum_{k=1}^{4} \Psi_k(x + \mu_k y)\right] \tag{11b}$$

$$\phi = \mathrm{Re}\left[\sum_{k=1}^{4} \phi_k(x + \mu_k y)\right] \tag{11c}$$

By eliminating ϕ in Eqs. (5a)–(5c), we can obtain relationship between F_k and Ψ_k as

$$\begin{aligned} \Psi_k &= \Lambda_k \frac{\mathrm{d}F_k}{\mathrm{d}z_k}, \quad \text{for } k = 1, 2, 4 \\ \Psi_k &= \frac{1}{\Lambda_k}\frac{\mathrm{d}F_k}{\mathrm{d}z_k}, \quad \text{for } k = 3 \end{aligned} \tag{12}$$

where $z_k = x + \mu_k y$ and

$$\Lambda_k = \begin{cases} -\dfrac{l_3(\mu_k)l_2^{**}(\mu_k) - l_3^*(\mu_k)l_2^*(\mu_k)}{l_2(\mu_k)l_2^{**}(\mu_k) - l_2^*(\mu_k)l_2^*(\mu_k)} & \text{for } k = 1,2 \\ -\dfrac{l_3(\mu_k)l_2^{**}(\mu_k) - l_3^*(\mu_k)l_2^*(\mu_k)}{l_4(\mu_k)l_2^{**}(\mu_k) - l_3^*(\mu_k)l_3^*(\mu_k)} & \text{for } k = 3 \\ -\dfrac{l_4(\mu_k)l_2^*(\mu_k) - l_3(\mu_k)l_3^*(\mu_k)}{l_3(\mu_k)l_2^*(\mu_k) - l_2(\mu_k)l_3^*(\mu_k)} & \text{for } k = 4 \end{cases} \tag{13}$$

Similarly, eliminating Ψ in Eqs. (5a)–(5c), it gives

$$\phi_k = \begin{cases} \Omega_k \dfrac{\mathrm{d}F_k}{\mathrm{d}z_k}, & \text{for } k = 1,2,3 \\ \dfrac{1}{\Omega_k}\dfrac{\mathrm{d}F_k}{\mathrm{d}z_k}, & \text{for } k = 4 \end{cases} \tag{14}$$

where

$$\Omega_k = \begin{cases} -\dfrac{l_2(\mu_k)l_3^*(\mu_k) - l_3(\mu_k)l_2^*(\mu_k)}{l_2(\mu_k)l_2^{**}(\mu_k) - l_2^*(\mu_k)l_2^*(\mu_k)} & \text{for } k = 1,2 \\ -\dfrac{l_4(\mu_k)l_2^*(\mu_k) - l_3(\mu_k)l_3^*(\mu_k)}{l_3^*(\mu_k)l_2^*(\mu_k) - l_3(\mu_k)l_2^{**}(\mu_k)} & \text{for } k = 3 \\ -\dfrac{l_2(\mu_k)l_3^*(\mu_k) - l_3(\mu_k)l_2^*(\mu_k)}{l_2(\mu_k)l_4(\mu_k) - l_3(\mu_k)l_3(\mu_k)} & \text{for } k = 4 \end{cases} \tag{15}$$

Therefore, Eqs. (11a)–(11c) can be rewritten as

$$F = 2\mathrm{Re}[F_1 + F_2 + F_3 + F_4] \tag{16a}$$

$$\Psi = 2\mathrm{Re}\left[\Lambda_1 F_1' + \Lambda_2 F_2' + \frac{1}{\Lambda_3}F_3' + \Lambda_4 F_4'\right] \tag{16b}$$

$$\phi = 2\mathrm{Re}\left[\Omega_1 F_1' + \Omega_2 F_2' + \Omega_3 F_3' + \frac{1}{\Omega_4}F_4'\right] \tag{16c}$$

By changing the notations

$$f_1 = F_1', \quad f_2 = F_2', \quad f_3 = \frac{1}{\Lambda_3}F_3', \quad f_4 = \frac{1}{\Omega_4}F_4' \tag{17}$$

Substituting Eqs. (16a)–(16c) into Eq. (4) and using the notations of Eq. (17), it gives

$$\sigma_x = 2\mathrm{Re}\left[\mu_1^2 f_1' + \mu_2^2 f_2' + \mu_3^2 \Lambda_3 f_3' + \mu_4^2 \Omega_4 f_4'\right] \tag{18a}$$

$$\sigma_y = 2\mathrm{Re}\left[f_1' + f_2' + \Lambda_3 f_3' + \Omega_4 f_4'\right] \tag{18b}$$

$$\tau_{xy} = -2\mathrm{Re}\left[\mu_1 f_1' + \mu_2 f_2' + \mu_3 \Lambda_3 f_3' + \mu_4 \Omega_4 f_4'\right] \tag{18c}$$

$$\tau_{xz} = 2\mathrm{Re}\left[\mu_1 \Lambda_1 f_1' + \mu_2 \Lambda_2 f_2' + \mu_3 f_3' + \mu_4 \Lambda_4 \Omega_4 f_4'\right] \tag{18d}$$

$$\tau_{yz} = -2\mathrm{Re}\left[\Lambda_1 f_1' + \Lambda_2 f_2' + f_3' + \Lambda_4 \Omega_4 f_4'\right] \tag{18e}$$

$$D_x = 2\mathrm{Re}\left[\mu_1\Omega_1 f_1' + \mu_2\Omega_2 f_2' + \mu_3\Lambda_3\Omega_3 f_3' + \mu_4 f_4'\right] \tag{18f}$$

$$D_y = -2\mathrm{Re}\left[\Omega_1 f_1' + \Omega_2 f_2' + \Lambda_3\Omega_3 f_3' + f_4'\right] \tag{18g}$$

where f_k denote the undetermined complex function; prime denotes the first derivative with respect to the argument z_k ($z_k = x + \mu_k y$).

Substituting Eqs. (18a)–(18g) into Eq. (2) and integrating, the results are

$$u = 2\mathrm{Re}\left[\sum_{k=1}^{4} u_k^* f_k\right] \tag{19a}$$

$$v = 2\mathrm{Re}\left[\sum_{k=1}^{4} v_k^* f_k\right] \tag{19b}$$

$$w = 2\mathrm{Re}\left[\sum_{k=1}^{4} w_k^* f_k\right] \tag{19c}$$

$$\Phi = 2\mathrm{Re}\left[\sum_{k=1}^{4} \Phi_k^* f_k\right] \tag{19d}$$

$$E_x = -2\mathrm{Re}\left[\sum_{k=1}^{4} \Phi_k^* f_k'\right] \tag{19e}$$

$$E_y = -2\mathrm{Re}\left[\sum_{k=1}^{4} \mu_k \Phi_k^* f_k'\right] \tag{19f}$$

where

$$u_k^* = \begin{cases} a_{11}\mu_k^2 + a_{12} - a_{14}\Lambda_k + a_{15}\mu_k\Lambda_k - a_{16}\mu_k + b_{11}\mu_k\Omega_k - b_{21}\Omega_k & \text{for } k = 1,2 \\ a_{11}\mu_k^2\Lambda_k + a_{12}\Lambda_k - a_{14} + a_{15}\mu_k - a_{16}\mu_k\Lambda_k + b_{11}\mu_k\Lambda_k\Omega_k - b_{21}\Lambda_k\Omega_k & \text{for } k = 3 \\ a_{11}\mu_k^2\Omega_k + a_{12}\Omega_k - a_{14}\Lambda_k\Omega_k + a_{15}\mu_k\Lambda_k\Omega_k - a_{16}\mu_k\Omega_k + b_{11}\mu_k - b_{21} & \text{for } k = 4 \end{cases} \tag{20a}$$

$$v_k^* = \begin{cases} a_{12}\mu_k + a_{22}/\mu_k - a_{24}\Lambda_k/\mu_k + a_{25}\Lambda_k - a_{26} + b_{12}\Omega_k - b_{22}\Omega_k/\mu_k & \text{for } k = 1,2 \\ a_{12}\mu_k\Lambda_k + a_{22}\Lambda_k/\mu_k - a_{24}/\mu_k + a_{25} - a_{26}\Lambda_k + b_{12}\Lambda_k\Omega_k - b_{22}\Lambda_k\Omega_k/\mu_k & \text{for } k = 3 \\ a_{12}\mu_k\Omega_k + a_{22}\Omega_k/\mu_k - a_{24}\Lambda_k\Omega_k/\mu_k + a_{25}\Lambda_k\Omega_k - a_{26}\Omega_k + b_{12} - b_{22}/\mu_k & \text{for } k = 4 \end{cases} \tag{20b}$$

$$w_k^* = \begin{cases} a_{14}\mu_k + a_{24}/\mu_k - a_{44}\Lambda_k/\mu_k + a_{45}\Lambda_k - a_{46} + b_{14}\Omega_k - b_{24}\Omega_k/\mu_k & \text{for } k = 1,2 \\ a_{14}\mu_k\Lambda_k + a_{24}\Lambda_k/\mu_k - a_{44}/\mu_k + a_{45} - a_{46}\Lambda_k + b_{14}\Lambda_k\Omega_k - b_{24}\Lambda_k\Omega_k/\mu_k & \text{for } k = 3 \\ a_{14}\mu_k\Omega_k + a_{24}\Omega_k/\mu_k - a_{44}\Lambda_k\Omega_k/\mu_k + a_{45}\Lambda_k\Omega_k - a_{46}\Omega_k + b_{14} - b_{24}/\mu_k & \text{for } k = 4 \end{cases} \tag{20c}$$

$$\Phi_k^* = \begin{cases} b_{11}\mu_k^2 + b_{12} - b_{14}\Lambda_k + b_{15}\mu_k\Lambda_k - b_{16}\mu_k - d_{11}\mu_k\Omega_k + d_{12}\Omega_k & \text{for } k = 1,2 \\ b_{11}\mu_k^2\Lambda_k + b_{12}\Lambda_k - b_{14} + b_{15}\mu_k - b_{16}\mu_k\Lambda_k - d_{11}\mu_k\Lambda_k\Omega_k + d_{12}\Lambda_k\Omega_k & \text{for } k = 3 \\ b_{11}\mu_k^2\Omega_k + b_{12}\Omega_k - b_{14}\Lambda_k\Omega_k + b_{15}\mu_k\Lambda_k\Omega_k - b_{16}\mu_k\Omega_k - d_{11}\mu_k + d_{12} & \text{for } k = 4 \end{cases} \tag{20d}$$

The integrating constants, which represent the rigid body motions (Chen and Yen, 1998), are ignored here.

3. Degenerate cases

Since the diagonal elements in Eq. (2) are non-zero, the polynomials $l_4(\mu)$, $l_2(\mu)$, $l_2^{**}(\mu)$ will not vanish. However, $l_3(\mu)$, $l_3^*(\mu)$, $l_2^*(\mu)$ may be zero for some symmetry properties of materials. Four decoupled categories can be deduced from the piezoelectric formulation under generalized plane deformation.

3.1. Class A: $l_3(\mu) = l_2^*(\mu) = 0$

If the material symmetry has the properties

$$\begin{aligned} &s_{14} = s_{15} = s_{24} = s_{25} = s_{46} = s_{56} = s_{34} = s_{35} = 0 \\ &g_{14} = g_{15} = g_{24} = g_{25} = g_{31} = g_{32} = g_{33} = g_{36} = 0 \\ &\beta_{13} = \beta_{23} = 0 \end{aligned} \tag{21}$$

Eq. (2) becomes

$$\begin{Bmatrix} \partial u/\partial x \\ \partial v/\partial y \\ \partial w/\partial y \\ \partial w/\partial x \\ \partial u/\partial y + \partial v/\partial x \\ \partial \Phi/\partial x \\ \partial \Phi/\partial y \end{Bmatrix} = \begin{bmatrix} a_{11} & a_{12} & 0 & 0 & a_{16} & b_{11} & b_{21} \\ a_{12} & a_{22} & 0 & 0 & a_{26} & b_{12} & b_{22} \\ 0 & 0 & a_{44} & a_{45} & 0 & 0 & 0 \\ 0 & 0 & a_{45} & a_{55} & 0 & 0 & 0 \\ a_{16} & a_{26} & 0 & 0 & a_{66} & b_{16} & b_{26} \\ b_{11} & b_{12} & 0 & 0 & b_{16} & -d_{11} & -d_{12} \\ b_{21} & b_{22} & 0 & 0 & b_{26} & -d_{12} & -d_{22} \end{bmatrix} \begin{Bmatrix} \sigma_x \\ \sigma_y \\ \tau_{yz} \\ \tau_{xz} \\ \tau_{xy} \\ D_x \\ D_y \end{Bmatrix} \tag{22}$$

One example of this case is that the material is symmetric with respect to the x–y plane. The formulation is decoupled into inplane and antiplane problems. The inplane problem consists of σ_x, σ_y, τ_{xy}, u, v, D_x, D_y, E_x, E_y and Φ, while antiplane problem consists of τ_{xz}, τ_{yz}, w.

Eqs. (10b) and (10e) yield

$$l_3(\mu) = l_2^*(\mu) = 0 \tag{23}$$

and Eq. (9) is reduced to be

$$l_2(\mu)\left[l_4(\mu)l_2^{**}(\mu) - l_3^*(\mu)l_3^*(\mu)\right] = 0 \tag{24}$$

or

$$l_4(\mu)l_2^{**}(\mu) - l_3^*(\mu)l_3^*(\mu) = 0 \tag{25a}$$

$$l_2(\mu) = 0 \tag{25b}$$

Eq. (25a) corresponds to inplane problem, and Eq. (25b) to antiplane problem. Under this condition, the mechanical and electrical fields are reduced to the following:

$$\sigma_x = 2\mathrm{Re}\left[\mu_1^2 f_1' + \mu_2^2 f_2' + \mu_4^2 \Omega_4 f_4'\right] \tag{26a}$$

$$\sigma_y = 2\mathrm{Re}\left[f_1' + f_2' + \Omega_4 f_4'\right] \tag{26b}$$

$$\tau_{xy} = -2\mathrm{Re}\left[\mu_1 f_1' + \mu_2 f_2' + \mu_4 \Omega_4 f_4'\right] \tag{26c}$$

$$D_x = 2\mathrm{Re}\left[\mu_1 \Omega_1 f_1' + \mu_2 \Omega_2 f_2' + \mu_4 f_4'\right] \tag{26d}$$

$$D_y = -2\mathrm{Re}\left[\Omega_1 f_1' + \Omega_2 f_2' + f_4'\right] \tag{26e}$$

$$u = 2\mathrm{Re}\left[u_1^* f_1 + u_2^* f_2 + u_4^* f_4\right] \tag{26f}$$

$$v = 2\mathrm{Re}\left[v_1^* f_1 + v_2^* f_2 + v_4^* f_4\right] \tag{26g}$$

$$\Phi = 2\mathrm{Re}\left[\Phi_1^* f_1 + \Phi_2^* f_2 + \Phi_4^* f_4\right] \tag{26h}$$

$$E_x = -2\mathrm{Re}\left[\Phi_1^* f_1' + \Phi_2^* f_2' + \Phi_4^* f_4'\right] \tag{26i}$$

$$E_y = -2\mathrm{Re}\left[\mu_1 \Phi_1^* f_1' + \mu_2 \Phi_2^* f_2' + \mu_4 \Phi_4^* f_4'\right] \tag{26j}$$

for inplane problem, and

$$\tau_{xz} = 2\mathrm{Re}\left[\mu_3 f_3'\right] \tag{27a}$$

$$\tau_{yz} = -2\mathrm{Re}\left[f_3'\right] \tag{27b}$$

$$w = 2\mathrm{Re}\left[w_3^* f_3'\right] \tag{27c}$$

for antiplane problem. If only the antiplane shear stresses τ_{xz} or τ_{yz} are applied, there is no electric response in the piezoelectric body.

Sosa (1991) has derived the formulations of this decoupled case and applied to the problem of an infinite piezoelectrical medium weakened by an elliptical hole. Later, Xu and Rajapakse (2000) used same formulations to solve the stress singularities in composite piezoelectric wedges and junctions.

3.2. Class B: $l_3(\mu) = l_3^*(\mu) = 0$

Some material symmetry will lead to $l_3(\mu) = l_3^*(\mu) = 0$. For example, hexagonal 6mm class symmetry is one of the cases. Eq. (2) has the form:

$$\begin{Bmatrix} \partial u/\partial x \\ \partial v/\partial y \\ \partial w/\partial y \\ \partial w/\partial x \\ \partial u/\partial y + \partial v/\partial x \\ \partial \Phi/\partial x \\ \partial \Phi/\partial y \end{Bmatrix} = \begin{bmatrix} a_{11} & a_{12} & 0 & 0 & 0 & 0 & 0 \\ a_{12} & a_{11} & 0 & 0 & 0 & 0 & 0 \\ 0 & 0 & a_{44} & 0 & 0 & 0 & b_{15} \\ 0 & 0 & 0 & a_{44} & 0 & b_{15} & 0 \\ 0 & 0 & 0 & 0 & a_{66} & 0 & 0 \\ 0 & 0 & 0 & b_{15} & 0 & -d_{11} & 0 \\ 0 & 0 & b_{15} & 0 & 0 & 0 & -d_{11} \end{bmatrix} \begin{Bmatrix} \sigma_x \\ \sigma_y \\ \tau_{yz} \\ \tau_{xz} \\ \tau_{xy} \\ D_x \\ D_y \end{Bmatrix} \tag{28}$$

where $a_{66} = 2(a_{11} - a_{12})$. It is observed that

$$\begin{aligned} a_{15} &= a_{14} = a_{56} = a_{25} = a_{46} = a_{24} = 0 \\ b_{11} &= b_{21} = b_{16} = b_{12} = b_{26} = b_{22} = 0 \end{aligned} \tag{29}$$

From Eqs. (10a)–(10f), it gives $l_3(\mu) = l_3^*(\mu) = 0$. Eq. (9) is simplified as

$$l_4(\mu)\left[l_2(\mu) l_2^{**}(\mu) - l_2^*(\mu) l_2^*(\mu)\right] = 0 \tag{30}$$

The mechanical and electrical fields can be rewritten as

$$\sigma_x = 2\mathrm{Re}\left[\mu_1^2 f_1' + \mu_2^2 f_2'\right] \tag{31a}$$

$$\sigma_y = 2\mathrm{Re}\left[f_1' + f_2'\right] \tag{31b}$$

$$\tau_{xy} = -2\mathrm{Re}\left[\mu_1 f_1' + \mu_2 f_2'\right] \tag{31c}$$

$$u = 2\mathrm{Re}\left[u_1^* f_1 + u_2^* f_2\right] \tag{31d}$$

$$v = 2\mathrm{Re}\left[v_1^* f_1 + v_2^* f_2\right] \tag{31e}$$

$$\tau_{xz} = 2\mathrm{Re}\left[\mu_3 f_3' + \mu_4 \Lambda_4 \Omega_4 f_4'\right] \tag{32a}$$

$$\tau_{yz} = -2\mathrm{Re}\left[f_3' + \Lambda_4 \Omega_4 f_4'\right] \tag{32b}$$

$$w = 2\mathrm{Re}\left[w_3^* f_3' + w_4^* f_4'\right] \tag{32c}$$

$$D_x = 2\mathrm{Re}\left[\mu_3 \Lambda_3 \Omega_3 f_3' + \mu_4 f_4'\right] \tag{32d}$$

$$D_y = -2\mathrm{Re}\left[\Lambda_3 \Omega_3 f_3' + f_4'\right] \tag{32e}$$

$$\Phi = 2\mathrm{Re}\left[\Phi_3^* f_3 + \Phi_4^* f_4\right] \tag{32f}$$

$$E_x = -2\mathrm{Re}\left[\Phi_3^* f_3' + \Phi_4^* f_4'\right] \tag{32g}$$

$$E_y = -2\mathrm{Re}\left[\mu_3 \Phi_3^* f_3' + \mu_4 \Phi_4^* f_4'\right] \tag{32h}$$

The electro-elastic field is decoupled into the inplane elastic field $(\sigma_x, \sigma_y, \tau_{xy}, u, v)$ and the antiplane elastic field $(\tau_{xz}, \tau_{yz}, w)$ associated with inplane electrical field $(D_x, D_y, E_x, E_y, \Phi)$. If only in-plane stresses are applied, there is no electric response in the piezoelectric body.

The antiplane crack problems of this decoupled case have been extensively investigated in last decade, such as Shindo et al. (1996, 1997) and Narita and Shindo (1998, 1999). The poling direction is along the z-axis.

3.3. Class C: No piezoelectric effect ($l_3^*(\mu) = l_2^*(\mu) = 0$)

For some crystal symmetry, such as orthotropic material (orthorhombic mmm class), the piezoelectric effect is not exhibited. The piezoelectric constants g_{ij} and hence $l_3^*(\mu)$, $l_2^*(\mu)$ are zero. Eq. (9) becomes

$$l_2^{**}(\mu)[l_4(\mu) l_2(\mu) - l_3(\mu) l_3(\mu)] = 0 \tag{33}$$

or

$$l_4(\mu) l_2(\mu) - l_3(\mu) l_3(\mu) = 0 \tag{34a}$$

$$l_2^{**}(\mu) = 0 \tag{34b}$$

Eqs. (34a) and (34b) correspond to mechanical and electrical responses, respectively. Also, Eq. (13) is reduced to the following form

$$\Lambda_k = \begin{cases} -\dfrac{l_3(\mu_k)}{l_2(\mu_k)} & \text{for } k = 1, 2 \\ -\dfrac{l_3(\mu_k)}{l_4(\mu_k)} & \text{for } k = 3 \end{cases} \tag{35}$$

The functions $\Omega_1(\mu_1)$, $\Omega_2(\mu_2)$, $\Omega_4(\mu_4)$, $\Lambda_3(\mu_3)\Omega_3(\mu_3)$ and $\Lambda_4(\mu_4)\Omega_4(\mu_4)$ in Eqs. (18a)–(18g) vanish. The mechanical and electrical fields are then

$$\sigma_x = 2\mathrm{Re}\left[\mu_1^2 f_1' + \mu_2^2 f_2' + \mu_3^2 \Lambda_3 f_3'\right] \tag{36a}$$

$$\sigma_y = 2\mathrm{Re}\left[f_1' + f_2' + \Lambda_3 f_3'\right] \tag{36b}$$

$$\tau_{xy} = -2\mathrm{Re}\left[\mu_1 f_1' + \mu_2 f_2' + \mu_3 \Lambda_3 f_3'\right] \tag{36c}$$

$$\tau_{xz} = 2\mathrm{Re}\left[\mu_1 \Lambda_1 f_1' + \mu_2 \Lambda_2 f_2' + \mu_3 f_3'\right] \tag{36d}$$

$$\tau_{yz} = -2\mathrm{Re}\left[\Lambda_1 f_1' + \Lambda_2 f_2' + f_3'\right] \tag{36e}$$

$$u = 2\mathrm{Re}\left[u_1^* f_1 + u_2^* f_2 + u_3^* f_3\right] \tag{36f}$$

$$v = 2\mathrm{Re}\left[v_1^* f_1 + v_2^* f_2 + v_3^* f_3\right] \tag{36g}$$

$$w = 2\mathrm{Re}\left[w_1^* f_1 + w_2^* f_2 + w_3^* f_3\right] \tag{36h}$$

$$D_x = 2\mathrm{Re}\left[\mu_4 f_4'\right] \tag{37a}$$

$$D_y = -2\mathrm{Re}\left[f_4'\right] \tag{37b}$$

$$\Phi = 2\mathrm{Re}\left[\Phi_4^* f_4\right] \tag{37c}$$

$$E_x = -2\mathrm{Re}\left[\Phi_4^* f_4'\right] \tag{37d}$$

$$E_y = -2\mathrm{Re}\left[\mu_4 \Phi_4^* f_4'\right] \tag{37e}$$

The stresses and displacements are exactly the same as the formulations derived by Lekhnitskii (1963). It can be seen that the mechanical and electrical responses are decoupled. Now, the reduced material constants in Eq. (2) become

$$a_{ij} = s_{ij} - \frac{s_{i3}s_{j3}}{s_{33}} \tag{38a}$$

$$b_{ij} = 0 \tag{38b}$$

$$d_{ij} = \beta_{ij} - \frac{\beta_{i3}\beta_{j3}}{\beta_{33}} \tag{38c}$$

3.4. Class D: $l_3(\mu) = l_3^*(\mu) = l_2^*(\mu) = 0$

One example of this case is that the principal axes of the orthotropic material are placed in the x–y plane or along the z-axis. Eq. (9) is simplified as

$$l_4(\mu) l_2(\mu) l_2^{**}(\mu) = 0 \tag{39}$$

The problem is decoupled into three parts. They are (a) $l_4(\mu) = 0$: the inplane case for mechanical response $(\sigma_x, \sigma_y, \tau_{xy}, u, v)$; (b) $l_2(\mu) = 0$: the antiplane case for mechanical response $(\tau_{xz}, \tau_{yz}, w)$ and (c) $l_2^{**}(\mu) = 0$: the inplane case for electrical response $(D_x, D_y, E_x, E_y, \Phi)$. The physical quantities are given as follows:

$$\sigma_x = 2\mathrm{Re}\left[\mu_1^2 f_1' + \mu_2^2 f_2'\right] \tag{40a}$$

$$\sigma_y = 2\mathrm{Re}\left[f_1' + f_2'\right] \tag{40b}$$

$$\tau_{xy} = -2\mathrm{Re}\left[\mu_1 f_1' + \mu_2 f_2'\right] \tag{40c}$$

$$u = 2\mathrm{Re}\left[u_1^* f_1 + u_2^* f_2\right] \tag{40d}$$

$$v = 2\mathrm{Re}\left[v_1^* f_1 + v_2^* f_2\right] \tag{40e}$$

$$\tau_{xz} = 2\mathrm{Re}\left[\mu_3 f_3'\right] \tag{41a}$$

$$\tau_{yz} = -2\mathrm{Re}\left[f_3'\right] \tag{41b}$$

$$w = 2\mathrm{Re}\left[w_3^* f_3\right] \tag{41c}$$

$$D_x = 2\mathrm{Re}\left[\mu_4 f_4'\right] \tag{42a}$$

$$D_y = -2\mathrm{Re}\left[f_4'\right] \tag{42b}$$

$$\Phi = 2\mathrm{Re}\left[\Phi_4^* f_4\right] \tag{42c}$$

$$E_x = -2\mathrm{Re}\left[\Phi_4^* f_4'\right] \tag{42d}$$

$$E_y = -2\mathrm{Re}\left[\mu_4 \Phi_4^* f_4'\right] \tag{42e}$$

4. Applications to wedge problems

The eigenfunction expansion method is widely used to compute the stress singularity order of the wedge problems. The potential functions $f_k(z_k)$ in the physical quantities of Eqs. (18a)–(18g) are written in the form

$$f_k(z_k) = A_k z_k^{\lambda} + B_k \bar{z}_k^{\bar{\lambda}} \quad k = 1, \ldots, 4 \tag{43}$$

where A_k, B_k are unknown complex constants, λ is eigenvalue. It is convenient to express the physical quantities in polar coordinate when the boundary and continuity conditions on the edges or bonding interface are considered. The transformations of stresses, etc. from Cartesian coordinates to polar coordinates are as follows:

$$\sigma_\theta = n^2 \sigma_x + m^2 \sigma_y - 2mn\tau_{xy} \tag{44a}$$

$$\tau_{r\theta} = -mn\sigma_x + mn\sigma_y + \left(m^2 - n^2\right)\tau_{xy} \tag{44b}$$

$$\tau_{\theta z} = -n\tau_{xz} + m\tau_{yz} \tag{44c}$$

$$D_\theta = -nD_x + mD_y \tag{44d}$$

where $m = \cos\theta$ and $n = \sin\theta$.

4.1. Boundary and continuity conditions

Due to the intrinsic electric coupling effect, the sensors and actuators in smart structures often have several composite wedges involving piezoelectric materials. Fig. 2 shows a two-material wedge system. The x-axis of the coordinate system xyz is placed along bonded surface. It makes angle θ_1 with the global coordinate system XYZ. The wedge angles θ_2 and θ_3 are defined in XYZ system. For convenience, material 1 is always referred to as piezoelectric material and material 2 may be piezoelectric material, composite material or isotropic material (conductor). In the case of generalized plane deformation, all possible boundary conditions are described as follows.

a. The edge of piezoelectric material

Traction free: $\sigma_\theta = \tau_{r\theta} = \tau_{\theta z} = 0$ (45a)

Electrically open: $D_\theta = 0$ (45b)

b. The edge of composite or conductor material

Traction free: $\sigma_\theta = \tau_{r\theta} = \tau_{\theta z} = 0$ (46)

c. The continuity conditions at the piezoelectric–piezoelectric interface

Continuity of stresses: $\sigma_\theta^{(1)} = \sigma_\theta^{(2)},\ \tau_{r\theta}^{(1)} = \tau_{r\theta}^{(2)},\ \tau_{\theta z}^{(1)} = \tau_{\theta z}^{(2)}$ (47a)

Continuity of displacements: $u^{(1)} = u^{(2)},\ v^{(1)} = v^{(2)},\ w^{(1)} = w^{(2)}$ (47b)

Continuity of electric displacements: $D_\theta^{(1)} = D_\theta^{(2)}$ (47c)

Continuity of electric potential: $\Phi^{(1)} = \Phi^{(2)}$ (47d)

The superscripts 1 and 2 denote materials 1 and 2, respectively.

d. Continuity conditions at the piezoelectric–composite interface

Continuity of stresses: $\sigma_\theta^{(1)} = \sigma_\theta^{(2)},\ \tau_{r\theta}^{(1)} = \tau_{r\theta}^{(2)},\ \tau_{\theta z}^{(1)} = \tau_{\theta z}^{(2)}$ (48a)

Continuity of displacements: $u^{(1)} = u^{(2)},\ v^{(1)} = v^{(2)},\ w^{(1)} = w^{(2)}$ (48b)

Electric insulation condition for composites: $D_\theta^{(1)} = 0$ (48c)

The superscripts 1 and 2 denote the piezoelectric material and composite material, respectively.

e. Continuity conditions at the piezoelectric–conductor interface

Continuity of stresses: $\sigma_\theta^{(1)} = \sigma_\theta^{(2)},\ \tau_{r\theta}^{(1)} = \tau_{r\theta}^{(2)},\ \tau_{\theta z}^{(1)} = \tau_{\theta z}^{(2)}$ (49a)

Continuity of displacements: $u^{(1)} = u^{(2)},\ v^{(1)} = v^{(2)},\ w^{(1)} = w^{(2)}$ (49b)

Ideal electric conductor condition: $\Phi^{(1)} = 0$ (49c)

The superscripts 1 and 2 denote the piezoelectric material and conductor material, respectively.

The boundary or continuity conditions can be combined to form different wedge problems. For example, the boundary and continuity conditions of piezoelectric–composite wedge are Eqs. (45a), (45b), (46), (48a)–(48c). These 14 boundary and continuity conditions can be written as

$$[M]\{X\} = \{0\} \tag{50}$$

where $[M]$ is a 14×14 matrix and $\{X\}$ is a 14×1 vector containing the unknown constants A_k and B_k, $k = 1, \ldots, 4$. The elements in $[M]$ are functions of material constants, wedge angle and eigenvalue λ. For a non-trivial solution, the determinant of $[M]$ must vanish, i.e.,

$$\det[M] = 0 \tag{51}$$

From Eq. (51), the eigenvalues in the interval $0 < \mathrm{Re}[\lambda] < 1$ can be solved numerically. The value $\mathrm{Re}[\lambda] - 1$ is called the stress singularity order. Table 1 lists the boundary and continuity conditions and the dimensions of matrix $[M]$.

As the generalized plane deformation problem is degenerated to classes A and B as described in Section 3, the dimension can be further reduced. For example, consider that two-piezoelectric material wedges are bonded together. The poling directions of both materials are in the x–y plane. The dimensions of the matrix $[M]$ are 12×12 and 4×4 for inplane and antiplane stress fields, respectively. Table 2 summaries the boundary and continuity conditions and the dimensions of matrix $[M]$ of all possible degenerated cases. If the wedge structure consists of composite material, the fiber orientation of the composite should be in the x–y plane or along the z-axis for all considered degenerate cases. Otherwise the problem is coupled. The boundary and continuity conditions listed in Table 1 should be employed instead of Table 2. Some examples of this type will be discussed later.

4.2. Numerical results and discussion

In this section, several examples are considered. Some of them have been investigated by the previous studies, such as Xu and Rajapakse (2000). The others are new results. Although some of the problems have been decoupled, we use the generalized plane deformation formulation to solve the eigenvalue. The boundary conditions are listed in Table 1. The materials used in the following calculation contain PZT-4,

Table 1
The boundary and continuity conditions and the dimension of the characteristic determinant under generalized plane deformation

Wedge type	Boundary and continuity conditions	Dimension of characteristic determinant
One-piezoelectric wedge	$\sigma_\theta = \tau_{r\theta} = \tau_{\theta z} = D_\theta = 0$ at both edges	8×8
Two-piezoelectric wedge	$\sigma_\theta = \tau_{r\theta} = \tau_{\theta z} = D_\theta = 0$ at $\theta = \theta_2, \theta_3$ $\sigma_\theta^{(1)} = \sigma_\theta^{(2)},\ \tau_{r\theta}^{(1)} = \tau_{r\theta}^{(2)},\ \tau_{\theta z}^{(1)} = \tau_{\theta z}^{(2)},\ u^{(1)} = u^{(2)},\ v^{(1)} = v^{(2)},$ $w^{(1)} = w^{(2)},\ D_\theta^{(1)} = D_\theta^{(2)},\ \Phi^{(1)} = \Phi^{(2)}$ at $\theta = \theta_1$	16×16
Piezoelectric–composite wedge	$\sigma_\theta = \tau_{r\theta} = \tau_{\theta z} = D_\theta = 0$ at $\theta = \theta_2$ $\sigma_\theta = \tau_{r\theta} = \tau_{\theta z} = 0$ at $\theta = \theta_3$ $\sigma_\theta^{(1)} = \sigma_\theta^{(2)},\ \tau_{r\theta}^{(1)} = \tau_{r\theta}^{(2)},\ \tau_{\theta z}^{(1)} = \tau_{\theta z}^{(2)},\ u^{(1)} = u^{(2)},\ v^{(1)} = v^{(2)},\ w^{(1)} = w^{(2)},\ D_\theta^{(1)} = 0$ at $\theta = \theta_1$	14×14
Piezoelectric–conductor wedge	$\sigma_\theta = \tau_{r\theta} = \tau_{\theta z} = D_\theta = 0$ at $\theta = \theta_2$ $\sigma_\theta = \tau_{r\theta} = \tau_{\theta z} = 0$ at $\theta = \theta_3$ $\sigma_\theta^{(1)} = \sigma_\theta^{(2)},\ \tau_{r\theta}^{(1)} = \tau_{r\theta}^{(2)},\ \tau_{\theta z}^{(1)} = \tau_{\theta z}^{(2)},\ u^{(1)} = u^{(2)},\ v^{(1)} = v^{(2)},\ w^{(1)} = w^{(2)},\ \Phi^{(1)} = 0$ at $\theta = \theta_1$	14×14

Table 2
The boundary and continuity conditions and the dimension of the characteristic determinant of two degenerate cases for various wedge types

Wedge type	Degenerate cases		Boundary and continuity conditions	Dimension of characteristic determinant
One-piezoelectric wedge	Poling: x–y plane	Inplane	$\sigma_\theta = \tau_{r\theta} = D_\theta = 0$ at both edges	6×6
		Antiplane	$\tau_{\theta z} = 0$ at both edges	2×2
	Poling: z-axis	Inplane	$\sigma_\theta = \tau_{r\theta} = 0$ at both edges	4×4
		Antiplane	$\tau_{\theta z} = D_\theta = 0$ at both edges	4×4
Two-piezoelectric wedge	Poling: x–y plane	Inplane	$\sigma_\theta = \tau_{r\theta} = D_\theta = 0$ at $\theta = \theta_2, \theta_3$ $\sigma_\theta^{(1)} = \sigma_\theta^{(2)}$, $\tau_{r\theta}^{(1)} = \tau_{r\theta}^{(2)}$, $u^{(1)} = u^{(2)}$, $v^{(1)} = v^{(2)}$, $D_\theta^{(1)} = D_\theta^{(2)}$, $\Phi^{(1)} = \Phi^{(2)}$ at $\theta = \theta_1$	12×12
		Antiplane	$\tau_{\theta z} = 0$ at $\theta = \theta_2, \theta_3$ $\tau_{\theta z}^{(1)} = \tau_{\theta z}^{(2)}$, $w^{(1)} = w^{(2)}$ at $\theta = \theta_1$	4×4
	Poling: z-axis	Inplane	$\sigma_\theta = \tau_{r\theta} = 0$ at $\theta = \theta_2, \theta_3$ $\sigma_\theta^{(1)} = \sigma_\theta^{(2)}$, $\tau_{r\theta}^{(1)} = \tau_{r\theta}^{(2)}$, $u^{(1)} = u^{(2)}$, $v^{(1)} = v^{(2)}$ at $\theta = \theta_1$	8×8
		Antiplane	$\tau_{\theta z} = D_\theta = 0$ at $\theta = \theta_2, \theta_3$ $\tau_{\theta z}^{(1)} = \tau_{\theta z}^{(2)}$, $w^{(1)} = w^{(2)}$, $D_\theta^{(1)} = D_\theta^{(2)}$, $\Phi^{(1)} = \Phi^{(2)}$ at $\theta = \theta_1$	8×8
Piezoelectric–composite wedge	Poling: x–y plane	Inplane	$\sigma_\theta = \tau_{r\theta} = D_\theta = 0$ at $\theta = \theta_2$ $\sigma_\theta = \tau_{r\theta} = 0$ at $\theta = \theta_3$ $\sigma_\theta^{(1)} = \sigma_\theta^{(2)}$, $\tau_{r\theta}^{(1)} = \tau_{r\theta}^{(2)}$, $u^{(1)} = u^{(2)}$, $v^{(1)} = v^{(2)}$, $D_\theta^{(1)} = 0$ at $\theta = \theta_1$	10×10
		Antiplane	$\tau_{\theta z} = 0$ at $\theta = \theta_2, \theta_3$ $\tau_{\theta z}^{(1)} = \tau_{\theta z}^{(2)}$, $w^{(1)} = w^{(2)}$ at $\theta = \theta_1$	4×4
	Poling: z-axis	Inplane	$\sigma_\theta = \tau_{r\theta} = 0$ at $\theta = \theta_2, \theta_3$ $\sigma_\theta^{(1)} = \sigma_\theta^{(2)}$, $\tau_{r\theta}^{(1)} = \tau_{r\theta}^{(2)}$, $u^{(1)} = u^{(2)}$, $v^{(1)} = v^{(2)}$ at $\theta = \theta_1$	8×8
		Antiplane	$\tau_{\theta z} = D_\theta = 0$ at $\theta = \theta_2$, $\tau_{\theta z} = 0$ at $\theta = \theta_3$ $\tau_{\theta z}^{(1)} = \tau_{\theta z}^{(2)}$, $w^{(1)} = w^{(2)}$, $D_\theta^{(1)} = 0$ at $\theta = \theta_1$	6×6
Piezoelectric–conductor wedge	Poling: x–y plane	Inplane	$\sigma_\theta = \tau_{r\theta} = D_\theta = 0$ at $\theta = \theta_2$ $\sigma_\theta = \tau_{r\theta} = 0$ at $\theta = \theta_3$ $\sigma_\theta^{(1)} = \sigma_\theta^{(2)}$, $\tau_{r\theta}^{(1)} = \tau_{r\theta}^{(2)}$, $u^{(1)} = u^{(2)}$, $v^{(1)} = v^{(2)}$, $\Phi^{(1)} = 0$ at $\theta = \theta_1$	10×10
		Antiplane	$\tau_{\theta z} = 0$ at $\theta = \theta_2, \theta_3$ $\tau_{\theta z}^{(1)} = \tau_{\theta z}^{(2)}$, $w^{(1)} = w^{(2)}$ at $\theta = \theta_1$	4×4
	Poling: z-axis	Inplane	$\sigma_\theta = \tau_{r\theta} = 0$ at $\theta = \theta_2, \theta_3$ $\sigma_\theta^{(1)} = \sigma_\theta^{(2)}$, $\tau_{r\theta}^{(1)} = \tau_{r\theta}^{(2)}$, $u^{(1)} = u^{(2)}$, $v^{(1)} = v^{(2)}$ at $\theta = \theta_1$	8×8
		Antiplane	$\tau_{\theta z} = D_\theta = 0$ at $\theta = \theta_2$, $\tau_{\theta z} = 0$ at $\theta = \theta_3$ $\tau_{\theta z}^{(1)} = \tau_{\theta z}^{(2)}$, $w^{(1)} = w^{(2)}$, $\Phi^{(1)} = 0$ at $\theta = \theta_1$	6×6

PZT-5, graphite/epoxy and the aluminum (as a conductor). The material properties of piezoceramics PZT-4 polarized in x-direction are given below (Xu and Rajapakse, 2000):

$$s_{11} = 7.9 \times 10^{-12}\ \mathrm{m^2/N}, \quad s_{33} = s_{22} = 10.9 \times 10^{-12}\ \mathrm{m^2/N}, \quad s_{12} = -2.1 \times 10^{-12}\ \mathrm{m^2/N},$$

$$s_{23} = -5.42 \times 10^{-12}\ \mathrm{m^2/N}, \quad s_{55} = 19.3 \times 10^{-12}\ \mathrm{m^2/N}, \quad s_{44} = 2(s_{22} - s_{23})$$

$$g_{11} = 26.1 \times 10^{-3}\ \mathrm{Vm/N}, \quad g_{13} = g_{12} = -11.1 \times 10^{-3}\ \mathrm{Vm/N}, \quad g_{35} = g_{26} = 39.4 \times 10^{-3}\ \mathrm{Vm/N}$$

$$\beta_{11} = 8.69 \times 10^{7}\ \mathrm{V^2/N}, \quad \beta_{33} = \beta_{22} = 7.66 \times 10^{7}\ \mathrm{V^2/N}$$

For PZT-5, the properties are

$$s_{11} = 9.46 \times 10^{-12}\ \mathrm{m^2/N}, \quad s_{33} = s_{22} = 14.4 \times 10^{-12}\ \mathrm{m^2/N}, \quad s_{12} = -2.98 \times 10^{-12}\ \mathrm{m^2/N},$$
$$s_{23} = -7.71 \times 10^{-12}\ \mathrm{m^2/N}, \quad s_{55} = 25.2 \times 10^{-12}\ \mathrm{m^2/N}, \quad s_{44} = 2(s_{22} - s_{23})$$

$$g_{11} = 24.8 \times 10^{-3}\ \mathrm{Vm/N}, \quad g_{13} = g_{12} = -11.4 \times 10^{-3}\ \mathrm{Vm/N}, \quad g_{35} = g_{26} = 38.2 \times 10^{-3}\ \mathrm{Vm/N}$$

$$\beta_{11} = 6.65 \times 10^{7}\ \mathrm{V^2/N}, \quad \beta_{33} = \beta_{22} = 6.53 \times 10^{7}\ \mathrm{V^2/N}$$

The other constants not shown here are all zero. If the poling direction is not along the x-axis, the coordinate transformation should be applied. The material properties of graphite/epoxy are (Xu and Rajapakse, 2000):

$$E_x = 132.8\ \mathrm{GPa}, \quad E_y = 10.76\ \mathrm{GPa}, \quad E_z = 10.96\ \mathrm{GPa}$$

$$G_{xy} = G_{xz} = 5.65\ \mathrm{GPa}, \quad G_{yz} = 3.61\ \mathrm{GPa}$$

$$v_{xy} = v_{xz} = 0.24, \quad v_{yz} = 0.49$$

The Young's modulus and Poisson ratio of the aluminum are $E = 68.9$ GPa and $v = 0.25$, respectively.

Before going into detail discussion, the validation of this approach will be examined first. Firstly, consider a PZT-4 wedge with wedge angle 270°. The poling direction is along the y-axis. The boundary conditions are traction free ($\sigma_\theta = \tau_{r\theta} = 0$) and electrically insulated ($D_\theta = 0$) at both edges. Using the formulations of Xu and Rajapakse (2000), the authors compute the singularity orders as $\mathrm{Re}[\lambda - 1] = -0.4426537$, -0.3154704 and -0.04257704, respectively. Based on this approach of generalized plane deformation, the boundary conditions are $\sigma_\theta = \tau_{r\theta} = \tau_{\theta z} = D_\theta = 0$ at both edges. The computed orders are exactly the same as those of Xu and Rajapakse (2000) for inplane field. In addition, the singularity order of antiplane field can also be obtained simultaneously, i.e. -0.3194601.

The second case is that two-piezoelectric (PZT-4 and PZT-5) wedges with wedge angles 180° and 90° are bonded together. The poling direction of the first material (PZT-4) makes 45° with the y-axis counterclockwise and that of the second material (PZT-5) is along the y-axis. The authors used Xu's formulations and got $\mathrm{Re}[\lambda - 1] = -0.4529005$, -0.3537674, and -0.1079129. Based on the formulations of this paper, the boundary and continuity conditions are listed in Table 1. The dimension of matrix $[M]$ is 16×16. Again, the computed orders of inplane field are exactly the same as the Xu's results. The antiplane stress singularity order is -0.3105615.

The third case is the piezoelectric-graphite/epoxy wedges. The wedge angles of piezoelectric and graphite/epoxy wedges are 180° and 90°, respectively. The poling of the PZT-4 is along the y-axis and the fiber direction of graphite/epoxy is along the x-axis. If the formulations of Xu and Rajapakse (2000) are used, the computed singularity orders are -0.34997889 and -0.022600370. This case has been discussed as an example in Section 4.1. The boundary and continuity conditions form a 14×14 matrix $[M]$. The computed orders of inplane field are again exactly the same. The antiplane stress singularity order is -0.17022616.

The last compared case is the piezoelectric–conductor wedges. The wedge angles of PZT-4 and aluminum are 180° and 90°, respectively. The poling of the PZT-4 is along the y-axis. The calculated results from Xu's and generalized plane deformation formulations are exactly the same, i.e. -0.5394357, -0.3828770, and -0.08007116, for inplane field. The order of the antiplane field is -0.3324470.

From the above discussion, it has been proved that the formulation of generalized plane deformation is correct as compared with the degenerated case A.

4.2.1. Degenerated case A

In this section, three examples are investigated. Although Xu and Rajapakse (2000) have discussed these problems, the results should be reexamined in detail.

4.2.1.1. Example 1: Piezoelectric–conductor wedge. Consider a piezoelectric (PZT-4)/aluminum wedge bonded to form a half plane. Both of the wedge angles are $\theta_2 = \theta_3 = 90°$. The boundary and continuity conditions are listed in Table 2. The dimensions of the decoupled matrices are 10×10 for inplane field and 4×4 for antiplane field, respectively. In this case, the coordinate systems XYZ and xyz coincide and $\theta_1 = 0°$ defined in Fig. 2. The poling direction β is in the x–y plane and is measured from the y-axis counterclockwise. Fig. 3 shows the variations of the inplane (real and imaginary parts) and antiplane stress singularity orders with the poling direction β. All of the orders are much weaker than the square root singularity. The singularity orders are repeated as β is varied from $-180° < \beta < 0°$ to $0° < \beta < 180°$. There are two roots over some β regions. This figure is different from Fig. 7(a) of Xu and Rajapakse (2000). However, using Xu's formulations, the authors yielded the same results as Fig. 3 of this paper.

Also, the antiplane singular stress field disappears if the poling is directed in the intervals $-180° < \beta < -90°$ to $0° < \beta < 90°$.

Consider another example where an aluminum wedge bonded to a PZT-4 half plane (Fig. 4). The poling directs along the y-axis (and so the Y-axis). The variations of the inplane and antiplane singularity orders with wedge angle θ_3 are plotted in Fig. 4. There are three roots for inplane field and the first root is stronger than -0.5. When θ_3 approaches 0°, the problem is reduced to a half plane of PZT-4 medium. The order becomes -0.5. This phenomenon results from the assumptions made on the boundary edges and interface, i.e. $D_\theta = 0$ on the free edge and $\Phi = 0$ on the interface. As $\theta_3 = 0°$, the apex of the wedge becomes the mixed point and singularity order is -0.5. In addition, when θ_3 is closed to 180°, the third root for inplane field is different from the plot of Xu (Fig. 7(b) in Xu's paper). Again, the authors have tried to use Xu's formulation and the results are identical to the present approach. For antiplane field, only elastic deformation is considered. As $\theta_3 = 0$, the wedge becomes a half plane with no singularity. The bonded wedge forms a crack for $\theta_3 = 180°$ and the singularity order is -0.5.

4.2.1.2. Example 2: Piezoelectric-graphite/epoxy wedge. Fig. 5 shows a graphite/epoxy wedge bonded on the piezoelectric (PZT-4) half plane. The interface is insulated electrically. The dimension of the matrix $[M]$ is 14×14 listed in Table 1. The inplane and antiplane singularity orders can be obtained simultaneously. The poling of piezoeceramic and the fiber of graphite/epoxy are directed along the y- and x-axis, respectively. Fig. 5 plots the inplane (real and imaginary parts) and antiplane singularity orders. Comparing with

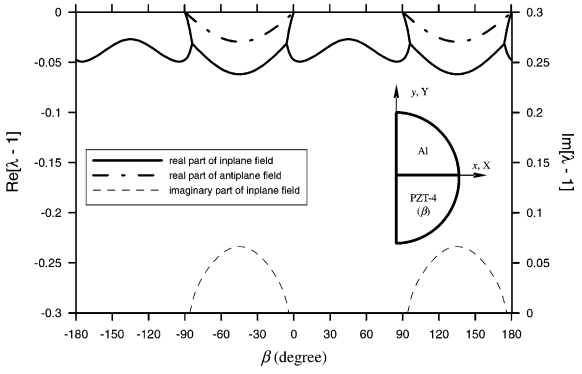

Fig. 3. The variation of stress singularities of a piezoelectric–conductor wedge with $\theta_2 = \theta_3 = 90°$.

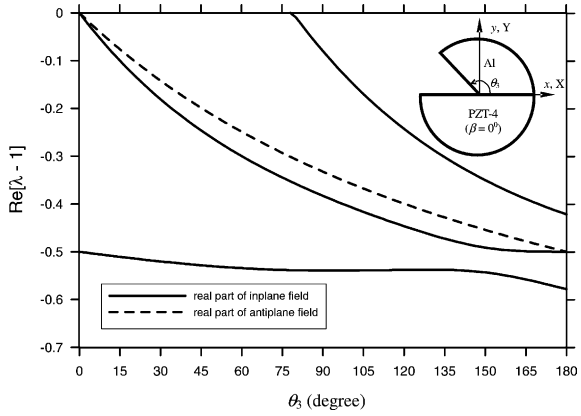

Fig. 4. The variations of singularity orders for an aluminum wedge bonded to a PZT-4 half plane.

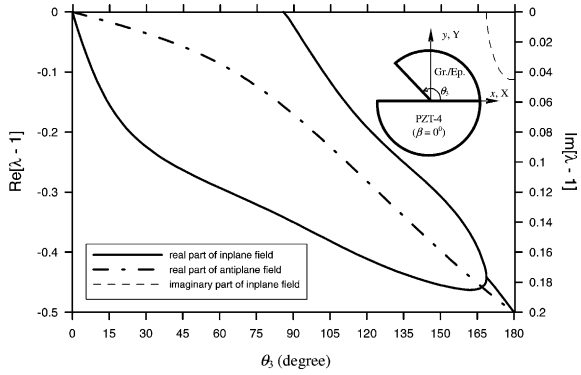

Fig. 5. The variations of stress singularity order for a graphite/epoxy wedge bonded to a PZT-4 half plane. The poling direction of PZT-4 is along y-axis, i.e., $\beta = 0°$.

Fig. 9(a) of Xu and Rajapakse (2000), the overall tendency is the same. However, when the wedge angle $\theta_3 \geqslant 165°$, some differences appear between the figures. Also, when $\theta_3 \geqslant 170°$, the two inplane roots become one complex root. The singularity orders in this example are reexamined by Xu's formulation. The results are consistent with the present approach. It is noted that, when the wedge angle θ_3 approaches zero, both of the inplane and antiplane orders are zero. This result matches the physical nature because both of the piezoelectric edge and the interface are insulated electrically. No stress singularity is expected if the graphite/epoxy wedge is removed.

4.2.1.3. Example 3: A debonded PZT-4-graphite/epoxy junction. Consider the last case shown in Fig. 6 of a debonded PZT-4-graphite/epoxy junction with electrically insulated interfaces. This case can be considered as a structure of two bonded wedges. The poling of PZT-4 and the fiber of graphite/epoxy are along the y- and x-axis, respectively. The variations of singularity orders with graphite/epoxy wedge angle $(\theta_3 - \theta_1)$ ranging from 0° to 360° are plotted in Fig. 6. This plot contains the inplane (real and imaginary parts) and antiplane singularity orders. Comparing with Fig. 9(b) of Xu and Rajapakse (2000), they are totally different. In Xu's plot, the angle $(\theta_3 - \theta_1)$ is in the interval between 90° and 270°. In the author's opinion, several inconsistencies can be pointed out in Xu's plot. From the physical standpoint, the wedge structure is

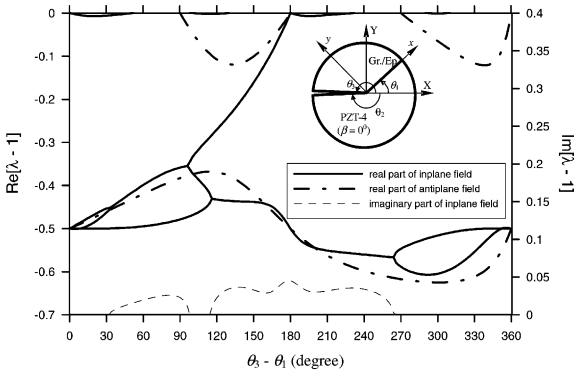

Fig. 6. The variation of stress singularities for a debonded PZT-4-graphite/epoxy junction.

not symmetric with respect to the interface. The distributions of the singularity order will not be symmetric with the angle $(\theta_3 - \theta_1) = 180°$. Also, as $(\theta_3 - \theta_1) = 90°$ or 270°, the singularity will not vanish. In addition, the values of the order will not change so abruptly as $(\theta_3 - \theta_1)$ is varied from 150° to 210°. Now, consider the results of this paper (Fig. 6). The plot covers the full range of angle $(\theta_3 - \theta_1)$ $(0° < (\theta_3 - \theta_1) < 360°)$ and is not symmetric with respect to $(\theta_3 - \theta_1)$ anymore. As $(\theta_3 - \theta_1)$ approaching 0°, the problem is reduced to the case of a piezoelectric medium containing a crack. The order approaches the classical square root type singularity. The singularity orders over the interval $0° < (\theta_3 - \theta_1) < 90°$ are very close to -0.5. In the other limiting case where $(\theta_3 - \theta_1)$ approaches 360°, the problem is reduced to the case of a composite medium containing a crack. Again, the order approaches the square root singularity. In these two limiting cases, the imaginary parts of the eigenvalue are zero. However, as $(\theta_3 - \theta_1) = 180°$, it becomes an interface crack and the order for inplane field is therefore complex. The stress near the crack tip will oscillate. It should be careful in the calculation of the eigenvalues from Eq. (51). Since the determinant of matrix $[M]$ contains the term z^λ which is a multiple-valued quantity, the principal argument should be defined in $-\pi < \mathrm{Arg}(z^\lambda) \leqslant \pi$. Due to this restriction, the positive X-axis has to be selected opposite to the debonding crack. When the boundary conditions are applied, the angles θ_2 and θ_3 (Fig. 2) of the boundary edges are input by $-179.99999°$ and 180°, respectively. Consider the singularity orders of antiplane field in Fig. 6. There are two roots in the interval $90° < (\theta_3 - \theta_1) < 180°$ and $270° < (\theta_3 - \theta_1) < 360°$. The first singularity orders are weaker or stronger than -0.5 when $(\theta_3 - \theta_1) < 180°$ or $(\theta_3 - \theta_1) > 180°$, respectively. As $(\theta_3 - \theta_1) = 0°$, 180°, and 360°, the classical square root singularity is assured.

4.2.2. Degenerated class B

In this class, the poling direction of the piezoelectric material is along the z-axis. The electro-elastic field is decoupled as mentioned in Section 3.2. In this section, four examples are investigated.

4.2.2.1. Example 1: Debonded piezoelectric bimaterial junction. Consider a debonded piezoelectric bimaterial junction shown in Fig. 7. The piezoelectric materials are PZT-4 and PZT-5. Both of these two materials are polarized along the z-axis. The interface along negative X-axis is fully debonded and electrically insulated. The x-axis, which makes angle θ_1 with the X-axis, is indicated as the bonded interface. Based on the plane strain deformation formulation, the dimension of the matrix $[M]$ is 16×16. The antiplane stress singularity orders are plotted in Fig. 7 as the angle θ_1 is varied. In general, there are three roots except when $\theta_1 = -180°$, $-90°$, 0°, 90°, and 180°. The cases of $\theta_1 = -180°$, 0° or 180° represent that a crack exists in a PZT-5 medium, at the PZT-4 and PZT-5 interface, or in a PZT-4 medium, respectively. All of the singularity orders in these three cases are -0.5. Since the material properties of PZT-4 and PZT-5 are very close,

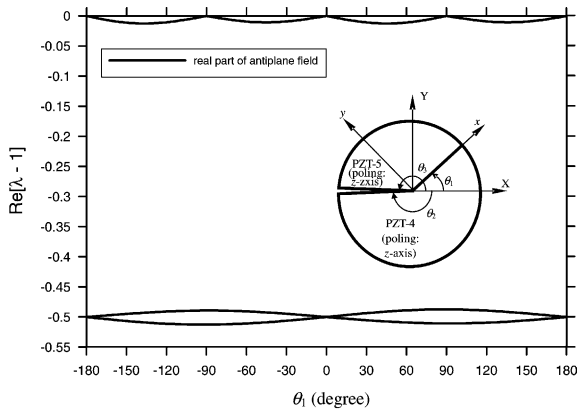

Fig. 7. The variation of stress singularity order for a debonded piezoelectric bimaterial junction.

all of the strongest and the second singularity orders are very close to -0.5, while that of the third orders are nearly zero. Although the difference is not significant, the variations of the order are not symmetric with respect to θ_1 For example as $\theta_1 = -90°$ or $90°$, the strongest order is -0.51257 or -0.51066, respectively.

4.2.2.2. Example 2: A graphite/epoxy wedge bonded on piezoelectric medium polarized along the z-axis. Fig. 8 shows a graphite/epoxy wedge fully bonded on the piezoelectric (PZT-4) half plane. The fiber of graphite/epoxy is along the x-axis. The interface is insulated electrically. The variations of inplane and antiplane singularity orders with wedge angle θ_3 are also shown in the figure. When compared with Fig. 5, it is noticed that the tendencies of these two figures are the same. The example discussed in Section 4.2.1.2 can be applied here.

4.2.2.3. Example 3: A graphite/epoxy quarter plane bonded to a piezoelectric quarter plane. Consider a half plane formed by a graphite/epoxy quarter plane and a piezoelectric quarter plan polarized along the z-axis. The graphite fiber lies in the X–Y plane and makes an angle α with the X-axis. The edge of the PZT-4 is traction free and electrically insulated, and traction free for graphite/epoxy edge. The boundary and continuity conditions are listed in Table 1, which form a 14×14 matrix $[M]$. Fig. 9 plots the variations of the inplane and antiplane singularity orders with the fiber orientation α. In general, the stress singularity orders of this problem are weaker than -0.12. For inplane stress field with no piezoelectric effect, the singularities disappear in three regions. For antiplane field, no stress singularity occurs when $\alpha \geqslant 90°$.

4.2.2.4. Example 4: An aluminum wedge bonded to a PZT-4 half plane. Consider an aluminum wedge bonded to a PZT-4 half plane shown in Fig. 10. There are two roots for antiplane stress field. One is varied with aluminum wedge angle θ_3 and the other remains at fixed value -0.5. These numerical results can also be obtained by using the Mellin transform on the antiplane stress function and inplane electric displacement function. Consider a two-material wedge bonded by a piezoelectric wedge with wedge angle θ_2 and a conductor wedge with wedge angle θ_3. The boundary and continuity conditions are the same as those in this example. The close form equation for the antiplane singularity order is (will be presented in a separate paper):

$$\cos(\lambda\theta_2)\left[\frac{\beta_{11}}{G}\cos(\lambda\theta_3)\sin(\lambda\theta_2) - (g_{15}g_{15} + \beta_{11}s_{44})\cos(\lambda\theta_2)\sin(\lambda\theta_3)\right] = 0 \tag{52}$$

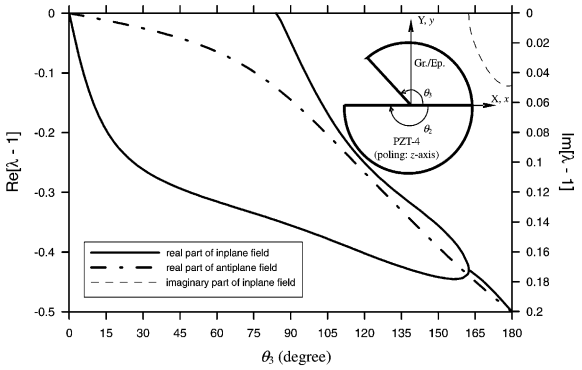

Fig. 8. The variation of stress singularity order for a graphite/epoxy wedge bonded to a PZT-4 half plane. The poling direction of PZT-4 is along z-axis.

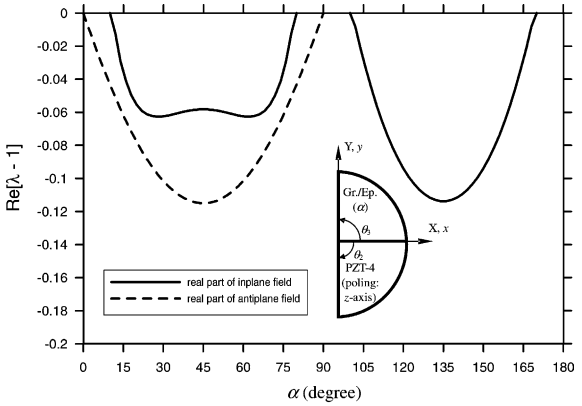

Fig. 9. The variation of singularity order for a half plane formed by a graphite/epoxy quarter plane and a piezoelectric quarter plane.

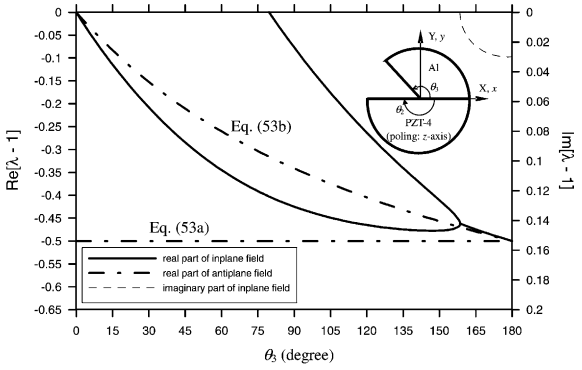

Fig. 10. The variation of inplane and antiplane singularity orders for an aluminum wedge bonded to a PZT-4 half plane. The poling direction of PZT-4 is along z-axis.

where G is the shear modulus of the conductor and λ is the eigenvalue. In this example $\theta_2 = \pi$ and $\theta_1 = 0$, i.e.

$$\cos(\lambda\pi) = 0 \tag{53a}$$

$$\left[\frac{\beta_{11}}{G}\cos(\lambda\theta_3)\sin(\lambda\pi) - (g_{15}g_{15} + \beta_{11}s_{44})\cos(\lambda\pi)\sin(\lambda\theta_3)\right] = 0 \tag{53b}$$

The solution of Eq. (53a) is $\lambda = 0.5$, which is independent of θ_3. The eigenvalues of Eq. (53b) are consistent with those in Fig. 10 for given material constants.

Since the aluminum is a conductor, the antiplane singularity order is kept at -0.5 when the wedge angle θ_3 approaches zero. Again, this is because that the apex of the wedge structure is a mixed boundary value point.

4.2.3. Generalized plane deformation problems (coupled cases)

In some engineering applications, the composite materials with fibers lying in x–z plane may be bonded to piezoelectric materials to act as a sensor or actuator. The materials possess no symmetry with respect to the x–y plane. The coupled formulation of Eq. (9) should be used to calculate the eigenvalues. Three examples of piezoelectric-graphite/epoxy wedges are investigated in this last section. PZT-4 is polarized along the y-axis. The orientation of the graphite fiber makes an angle γ with the x-axis.

4.2.3.1. Example 1: A graphite/epoxy quarter plane bonded to a piezoelectric quarter plane. Consider that a graphite/epoxy quarter plane and a piezoelectric (PZT-4) quarter plane are bonded together to form a half plane. The edge of the PZT-4 is traction free and electrically insulated. The edge of the graphite/epoxy is traction free. The interface is fully bonded and electrically insulated. Totally, there are 14 boundary and continuity conditions listed in Table 1 and the dimension of the matrix $[M]$ is 14×14. Fig. 11 plots the variations of the singularity order with the graphite fiber angle γ. As expected, it is symmetric with respect to $\gamma = 0°$. The stress singularity disappears when $\gamma \doteqdot 0°$ The strongest singularity occurs when the graphite fiber is orientated along the z-axis.

4.2.3.2. Example 2: A graphite/epoxy quarter plane bonded to a piezoelectric half plane. This example is the same as the previous one except that the PZT-4 wedge angle is 180°. Fig. 12 plots the variations of the singularity order with the graphite fiber angle γ. As expected again, it is symmetric with respect to $\gamma = 0°$. Generally there are three roots and the strongest singularity is $\doteqdot -0.35$ for all γ. No disappearance of stress singularity can be found in this case.

4.2.3.3. Example 3: A debonded PZT-4-graphite/epoxy junction ($\gamma = 90°$). Consider the last case of a debonded PZT-4-graphite/epoxy junction shown in Fig. 13. The graphite fiber is orientated along the z-axis and the poling direction of the PZT-4 is along the y-axis. Actually, the problem can be decoupled into inplane and antiplane stress fields. The inplane field takes into account the piezoelectric effect, but not the antiplane field. Fig. 13 plots the variations of the inplane (real and imaginary parts) and antiplane singularity orders with the graphite/epoxy wedge angle $(\theta_3 - \theta_1)$. For three special cases when $(\theta_3 - \theta_1) = 0°$, 180°, and 360°, the real parts of inplane and antiplane singularity orders are all -0.5. When the wedge angle $(\theta_3 - \theta_1) > 180°$, the orders are stronger than -0.5. Therefore, if the PZT-4 wedge angle is larger than the graphite wedge angle, the structure is more easily debonded.

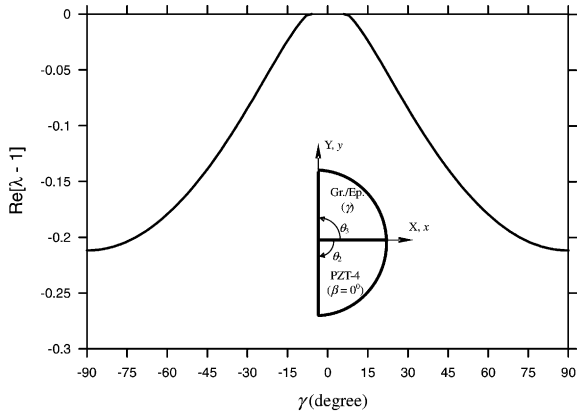

Fig. 11. The variation of stress singularities for a PZT-4-graphite/epoxy bonded wedge with wedge angle $\theta_2 = \theta_3 = 90°$.

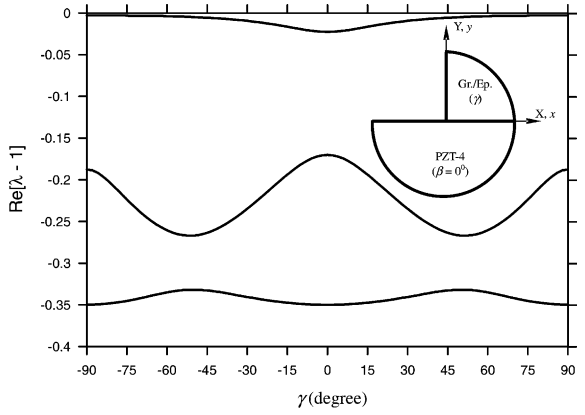

Fig. 12. The variation of stress singularity orders for a graphite/epoxy wedge bonded to a PZT-4 half plane.

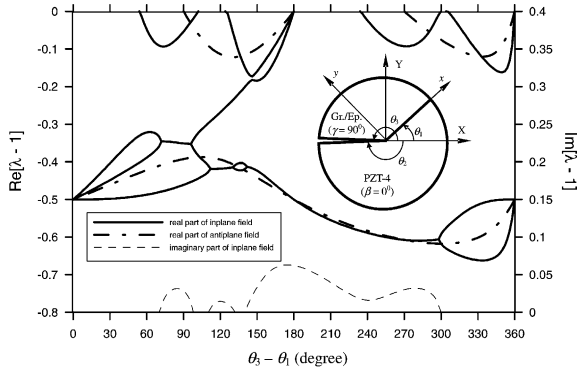

Fig. 13. The inplane and antiplane singularity orders for a debonded piezoelectric-graphite/epoxy junction.

5. Conclusions

A characteristic equation governing the electro-elastic singularities has been derived under the assumption of generalized plane deformation. From the eight-order polynomial equation, four categories of degenerated case can be deduced. Class A contains inplane piezoelastic field and antiplane anisotropic elastic field, while Class B contains inplane anisotropic elastic field and antiplane piezoelastic fields. Class C is equivalent to the Lekhnitskii's formulation of anisotropic elasticity and the electric potential field. The Lekhnitskii's formulation in Class D is simply decoupled into inplane and antiplane elastic fields. Several wedge problems bonded by PZT-4, PZT-5, graphite/epoxy or aluminum have been discussed to study the piezoelectric effect on the singular behavior. In Class A, some inconsistencies in Xu's paper are examined in detail. The results of Class B as well as coupled generalized plane deformation are new in this field. The conditions of weakest or vanishing singular stress fields can be determined by selecting the fiber orientation of the graphite/epoxy, the poling direction of the piezoelectric material, or the wedge angles. This can provide a useful guideline to design a reliable smart structure.

Appendix A. Derivation of Eq. (2) under generalized plane deformation formulations

The derivation of generalized plane deformation formulation starts with the assumption that ε_z is independent of z. By integrating the third row of Eq. (1), we have

$$w = zH_1(x,y) + W_0(x,y) \tag{A.1}$$

where w is the displacement in z-direction, W_0 is an arbitrary function of x, y and

$$H_1 = s_{13}\sigma_x + s_{23}\sigma_y + s_{33}\sigma_z + s_{34}\tau_{yz} + s_{35}\tau_{xz} + s_{36}\tau_{xy} + g_{13}D_x + g_{23}D_y + g_{33}D_z \tag{A.2}$$

After integrating the fourth and fifth rows of Eq. (1) and using Eq. (A.1), it gives

$$u = -\frac{z^2}{2}\frac{\partial H_1}{\partial x} + z\left(s_{15}\sigma_x + s_{25}\sigma_y + s_{35}\sigma_z + s_{45}\tau_{yz} + s_{55}\tau_{xz} + s_{56}\tau_{xy} + g_{15}D_x + g_{25}D_y + g_{35}D_z - \frac{\partial W_0}{\partial x}\right) + U_0(x,y) \tag{A.3a}$$

$$v = -\frac{z^2}{2}\frac{\partial H_1}{\partial y} + z\left(s_{14}\sigma_x + s_{24}\sigma_y + s_{34}\sigma_z + s_{44}\tau_{yz} + s_{45}\tau_{xz} + s_{46}\tau_{xy} + g_{14}D_x + g_{24}D_y + g_{34}D_z - \frac{\partial W_0}{\partial y}\right) + V_0(x,y) \tag{A.3b}$$

where U_0 and V_0 are arbitrary functions of x and y. It is noticed that displacements u, v, and w are functions of x, y, z. Substituting Eqs. (A.3a) and (A.3b) into the first, second and sixth row of Eq. (1) and using the strain-displacement relations, we get three equations where each contains z^2, z and z^0. By equating the coefficients of z^2, z and z^0 it gives

$$H_1 = s_{33}(Ax + By + C) \tag{A.4}$$

$$s_{15}\sigma_x + s_{25}\sigma_y + s_{35}\sigma_z + s_{45}\tau_{yz} + s_{55}\tau_{xz} + s_{56}\tau_{xy} + g_{15}D_x + g_{25}D_y + g_{35}D_z - \frac{\partial W_0}{\partial x} = -\bar{\theta}y + \omega_2 \tag{A.5a}$$

$$s_{14}\sigma_x + s_{24}\sigma_y + s_{34}\sigma_z + s_{44}\tau_{yz} + s_{45}\tau_{xz} + s_{46}\tau_{xy} + g_{14}D_x + g_{24}D_y + g_{34}D_z - \frac{\partial W_0}{\partial y} = \bar{\theta}x - \omega_1 \tag{A.5b}$$

$$\frac{\partial U_0}{\partial x} = s_{11}\sigma_x + s_{12}\sigma_y + s_{13}\sigma_z + s_{14}\tau_{yz} + s_{15}\tau_{xz} + s_{16}\tau_{xy} + g_{11}D_x + g_{21}D_y + g_{31}D_z \tag{A.6a}$$

$$\frac{\partial V_0}{\partial y} = s_{12}\sigma_x + s_{22}\sigma_y + s_{23}\sigma_z + s_{24}\tau_{yz} + s_{25}\tau_{xz} + s_{26}\tau_{xy} + g_{12}D_x + g_{22}D_y + g_{32}D_z \tag{A.6b}$$

$$\frac{\partial U_0}{\partial y} + \frac{\partial V_0}{\partial x} = s_{16}\sigma_x + s_{26}\sigma_y + s_{36}\sigma_z + s_{46}\tau_{yz} + s_{56}\tau_{xz} + s_{66}\tau_{xy} + g_{16}D_x + g_{26}D_y + g_{36}D_z \tag{A.6c}$$

where A, B, C, $\bar{\theta}$, ω_1 and ω_2 are arbitrary constants. Substituting Eq. (A.4) into Eq. (A.2), it gives

$$\sigma_z = Ax + By + C - \frac{1}{s_{33}}\left(s_{13}\sigma_x + s_{23}\sigma_y + s_{34}\tau_{yz} + s_{35}\tau_{xz} + s_{36}\tau_{xy} + g_{13}D_x + g_{23}D_y + g_{33}D_z\right) \tag{A.7}$$

Substituting Eqs. (A.5a), (A.5b) and (A.7) into Eqs. (A.1), (A.3a) and (A.3b), one has

$$u = \frac{-As_{33}}{2}z^2 - \bar{\theta}yz + U + \omega_2 z - \omega_3 y + u_0 \tag{A.8a}$$

$$v = \frac{-Bs_{33}}{2}z^2 + \bar{\theta}xz + V + \omega_3 x - \omega_1 z + v_0 \tag{A.8b}$$

$$w = (Ax + By + C)s_{33}z + W + \omega_1 y - \omega_2 x + w_0 \tag{A.8c}$$

where u_0, v_0, w_0 and ω_3 are arbitrary constants and

$$U = U_0 + \omega_3 y - u_0 \tag{A.9a}$$

$$V = V_0 - \omega_3 x - v_0 \tag{A.9b}$$

$$W = W_0 - \omega_1 y + \omega_2 x - w_0 \tag{A.9c}$$

Substituting Eq. (A.7) into Eqs. (A.6a)–(A.6c) and then into the seventh, eighth, ninth rows of Eq. (1), and using the relations Eqs. (A.9a)–(A.9c), it gives

$$\begin{Bmatrix} \partial U/\partial x \\ \partial V/\partial y \\ \partial W/\partial y \\ \partial W/\partial x \\ \partial U/\partial y + \partial V/\partial x \\ -E_x \\ -E_y \\ -E_z \end{Bmatrix} = \begin{bmatrix} \tilde{a}_{11} & \tilde{a}_{12} & \tilde{a}_{14} & \tilde{a}_{15} & \tilde{a}_{16} & \tilde{b}_{11} & \tilde{b}_{21} & \tilde{b}_{31} \\ \tilde{a}_{12} & \tilde{a}_{22} & \tilde{a}_{24} & \tilde{a}_{25} & \tilde{a}_{26} & \tilde{b}_{12} & \tilde{b}_{22} & \tilde{b}_{32} \\ \tilde{a}_{14} & \tilde{a}_{24} & \tilde{a}_{44} & \tilde{a}_{45} & \tilde{a}_{46} & \tilde{b}_{14} & \tilde{b}_{24} & \tilde{b}_{34} \\ \tilde{a}_{15} & \tilde{a}_{25} & \tilde{a}_{45} & \tilde{a}_{55} & \tilde{a}_{56} & \tilde{b}_{15} & \tilde{b}_{25} & \tilde{b}_{35} \\ \tilde{a}_{16} & \tilde{a}_{26} & \tilde{a}_{46} & \tilde{a}_{56} & \tilde{a}_{66} & \tilde{b}_{16} & \tilde{b}_{26} & \tilde{b}_{36} \\ \tilde{b}_{11} & \tilde{b}_{12} & \tilde{b}_{14} & \tilde{b}_{15} & \tilde{b}_{16} & -\tilde{d}_{11} & -\tilde{d}_{12} & -\tilde{d}_{13} \\ \tilde{b}_{21} & \tilde{b}_{22} & \tilde{b}_{24} & \tilde{b}_{25} & \tilde{b}_{26} & -\tilde{d}_{12} & -\tilde{d}_{22} & -\tilde{d}_{23} \\ \tilde{b}_{31} & \tilde{b}_{32} & \tilde{b}_{34} & \tilde{b}_{35} & \tilde{b}_{36} & -\tilde{d}_{13} & -\tilde{d}_{23} & -\tilde{d}_{33} \end{bmatrix} \begin{Bmatrix} \sigma_x \\ \sigma_y \\ \tau_{yz} \\ \tau_{xz} \\ \tau_{xy} \\ D_x \\ D_y \\ D_z \end{Bmatrix} + \begin{Bmatrix} s_{13}(Ax + By + C) \\ s_{23}(Ax + By + C) \\ s_{34}(Ax + By + C) - \bar{\theta}x - \omega_1 \\ s_{35}(Ax + By + C) + \bar{\theta}y + \omega_2 \\ s_{36}(Ax + By + C) \\ g_{13}(Ax + By + C) \\ g_{23}(Ax + By + C) \\ g_{33}(Ax + By + C) \end{Bmatrix} \tag{A.10}$$

where

$$\tilde{a}_{ij} = s_{ij} - \frac{s_{i3}s_{j3}}{s_{33}} \tag{A.11a}$$

$$\tilde{b}_{ij} = g_{ij} - \frac{s_{j3}g_{i3}}{s_{33}} \tag{A.11b}$$

$$\tilde{d}_{ij} = \beta_{ij} + \frac{g_{i3}g_{j3}}{s_{33}} \tag{A.11c}$$

It is noticed that u_0, v_0, w_0, ω_1, ω_2, ω_3 are rigid body motions; $\bar{\theta}$ is a twisting angle; A and B are parameters related to bending moments in the x–z and y–z planes; C is parameter related to external normal force P_z.

Assume that E_x, E_y and E_z are functions of x and y only. By definition, the relation between E_z and electric potential Φ is

$$E_z = -\frac{\partial \Phi}{\partial z} \tag{A.12}$$

By comparing Eq. (A.12) and the eighth row of Eq. (A.10), one has

$$\frac{\partial \Phi}{\partial z} = H_2(x,y) + g_{33}(Ax + By + C) \tag{A.13}$$

where

$$H_2 = \tilde{b}_{31}\sigma_x + \tilde{b}_{32}\sigma_y + \tilde{b}_{34}\tau_{yz} + \tilde{b}_{35}\tau_{xz} + \tilde{b}_{36}\tau_{xy} - \tilde{d}_{13}D_x - \tilde{d}_{23}D_y - \tilde{d}_{33}D_z \tag{A.14}$$

Integrating Eq. (A.13) with respect to z yields

$$\Phi = zH_2 + g_{33}z(Ax + By + C) + \Phi_0(x,y) \tag{A.15}$$

where Φ_0 is an arbitrary function of x and y. It is noticed that Φ is function of x, y and z. Since $E_x = -(\partial\Phi/\partial x)$ and $E_y = -(\partial\Phi/\partial y)$, the x- and y-components of the electric fields can be written as

$$E_x = -z\frac{\partial H_2}{\partial x} - Ag_{33}z - \frac{\partial \Phi_0}{\partial x} \tag{A.16a}$$

$$E_y = -z\frac{\partial H_2}{\partial y} - Bg_{33}z - \frac{\partial \Phi_0}{\partial y} \tag{A.16b}$$

Substituting Eqs. (A.16a) and (A.16b) into the sixth and seventh rows of (A.10) and then comparing the coefficients of z and z^0, we obtain

$$H_2 = -g_{33}(Ax + By + D) \tag{A.17}$$

$$\tilde{b}_{11}\sigma_x + \tilde{b}_{12}\sigma_y + \tilde{b}_{14}\tau_{yz} + \tilde{b}_{15}\tau_{xz} + \tilde{b}_{16}\tau_{xy} - \tilde{d}_{11}D_x - \tilde{d}_{12}D_y - \tilde{d}_{13}D_z + g_{13}(Ax + By + C) - \frac{\partial \Phi_0}{\partial x} = 0 \tag{A.18a}$$

$$\tilde{b}_{21}\sigma_x + \tilde{b}_{22}\sigma_y + \tilde{b}_{24}\tau_{yz} + \tilde{b}_{25}\tau_{xz} + \tilde{b}_{26}\tau_{xy} - \tilde{d}_{12}D_x - \tilde{d}_{22}D_y - \tilde{d}_{23}D_z + g_{23}(Ax + By + C) - \frac{\partial \Phi_0}{\partial y} = 0 \tag{A.18b}$$

where D is an arbitrary constant. It is noted that by substituting Eq. (17) into Eq. (15) and then using Eq. (A.12), we find that E_z is a constant. Substituting Eq. (A.17) into Eq. (A.14), we have

$$D_z = \frac{g_{33}}{\tilde{d}_{33}}(Ax + By + D) + \frac{1}{\tilde{d}_{33}}\left(\tilde{b}_{31}\sigma_x + \tilde{b}_{32}\sigma_y + \tilde{b}_{34}\tau_{yz} + \tilde{b}_{35}\tau_{xz} + \tilde{b}_{36}\tau_{xy} - \tilde{d}_{13}D_x - \tilde{d}_{23}D_y\right) \tag{A.19}$$

Substituting Eq. (A.19) into Eqs. (A.18a) and (A.18b) and then into the first five rows of Eq. (A.10), it yields

$$\begin{Bmatrix} \partial U/\partial x \\ \partial V/\partial y \\ \partial W/\partial y \\ \partial W/\partial x \\ \partial U/\partial y + \partial V/\partial x \\ \partial \Phi_0/\partial x \\ \partial \Phi_0/\partial y \end{Bmatrix} = \begin{bmatrix} a_{11} & a_{12} & a_{14} & a_{15} & a_{16} & b_{11} & b_{21} \\ a_{12} & a_{22} & a_{24} & a_{25} & a_{26} & b_{12} & b_{22} \\ a_{14} & a_{24} & a_{44} & a_{45} & a_{46} & b_{14} & b_{24} \\ a_{15} & a_{25} & a_{45} & a_{55} & a_{56} & b_{15} & b_{25} \\ a_{16} & a_{26} & a_{46} & a_{56} & a_{66} & b_{16} & b_{26} \\ b_{11} & b_{12} & b_{14} & b_{15} & b_{16} & -d_{11} & -d_{12} \\ b_{21} & b_{22} & b_{24} & b_{25} & b_{26} & -d_{12} & -d_{22} \end{bmatrix} \begin{Bmatrix} \sigma_x \\ \sigma_y \\ \tau_{yz} \\ \tau_{xz} \\ \tau_{xy} \\ D_x \\ D_y \end{Bmatrix} + \{\text{non-homogeneous terms}\} \tag{A.20}$$

where

$$a_{ij} = \tilde{a}_{ij} + \frac{\tilde{b}_{3i}\tilde{b}_{3j}}{\tilde{d}_{33}} \tag{A.21a}$$

$$b_{ij} = \tilde{b}_{ij} - \frac{\tilde{d}_{i3}\tilde{b}_{3j}}{\tilde{d}_{33}} \tag{A.21b}$$

$$d_{ij} = \tilde{d}_{ij} - \frac{\tilde{d}_{i3}\tilde{d}_{j3}}{\tilde{d}_{33}} \tag{A.21c}$$

In Eq. (A.20), the non-homogeneous terms are given as follows

$$s_{33}(Ax + By + C)\begin{Bmatrix} \alpha_1 \\ \alpha_2 \\ \alpha_4 \\ \alpha_5 \\ \alpha_6 \\ \xi_1 \\ \xi_2 \end{Bmatrix} + g_{33}(C - D)\begin{Bmatrix} \beta_1 \\ \beta_2 \\ \beta_4 \\ \beta_5 \\ \beta_6 \\ \eta_1 \\ \eta_2 \end{Bmatrix} + \begin{Bmatrix} 0 \\ 0 \\ -\bar{\theta}x - \omega_1 \\ \bar{\theta}y + \omega_2 \\ 0 \\ 0 \\ 0 \end{Bmatrix} \tag{A.22}$$

where D is a constant and

$$\begin{aligned} \alpha_i &= \frac{s_{i3}\beta_{33} + g_{3i}g_{33}}{s_{33}\beta_{33} + g_{33}^2}, \quad \beta_i = \frac{s_{i3}g_{33} - g_{3i}s_{33}}{s_{33}\beta_{33} + g_{33}^2} \\ \xi_i &= \frac{g_{i3}\beta_{33} - g_{33}\beta_{i3}}{s_{33}\beta_{33} + g_{33}^2}, \quad \eta_i = \frac{g_{i3}g_{33} + s_{33}\beta_{i3}}{s_{33}\beta_{33} + g_{33}^2} \end{aligned} \tag{A.23}$$

If we discard the rigid body motions u_0, v_0, w_0, ω_1, ω_2, ω_3 and the constants $\bar{\theta}$, A, B, C and D, the result is Eq. (2).

References

Barnett, D.M., Lothe, J., 1975. Dislocations and line charges in anisotropic piezoelectric insulators. Physica Status Solidi (b) 67, 105–111.

Bogy, D.B., 1971. Two edge-bonded elastic wedges of different materials and wedge angles under surface tractions. Journal of Applied Mechanics 35, 460–466.

Bogy, D.B., 1972. The plane solution for anisotropic elastic wedges under normal and shear loading. Journal of Applied Mechanics 39, 1103–1109.

Chen, H.P., 1998. Stress singularities in anisotropic multi-material wedges and junctions. International Journal of Solids and Structures 35, 1057–1073.

Chen, T., Lai, D., 1997. An exact correspondence between plane piezoelectricity and generalized plane strain in elasticity. Proceeding of Royal Society London A 453, 2689–2713.

Chen, T., Yen, W.J., 1998. Piezoelectric analogy of generalized torsion in anisotropic elasticity. Journal of Elasticity 49, 239–256.

Delale, F., 1984. Stress singularities in bonded anisotropic materials. International Journal of Solids and Structures 20, 31–40.

Gandhi, M.V., Thompson, B.S., 1992. Smart Materials and Structures. Chapman and Hall, UK.

Huang, T.F., Chen, W.H., 1994. On the free-edge stress singularity of general composite laminates under uniform axial strain. International Journal of Solids and Structures 31, 3139–3151.

Kuo, C.M., Barnett, D.M., 1991. Stress singularities of interfacial cracks in bonded piezoelectric half-spaces. In: Wu, J.J., Ting, T.C.T., Barnett, D.M. (Eds.), Modern Theory of Anisotropic Elasticity and Applications. SIAM, Philadelphia, pp. 33–50.

Lekhnitskii, S.G., 1963. Theory of Elasticity of an Anisotropic Elasticity body. Holden-Day, New York.

Ma, C.C., Hour, B.L., 1989. Analysis of dissimilar anisotropic wedges subjected to antiplane shear deformation. International Journal of Solids and Structures 25, 1295–1309.

Narita, F., Shindo, Y., 1998. Layered piezoelectric medium with interface crack under anti-plane shear. Theoretical and Applied Fracture Mechanics 30, 119–126.

Narita, F., Shindo, Y., 1999. The interface crack problem for bonded piezoelectric and orthotropic layers under antiplane shear loading. International Journal of Fracture 98, 87–101.

Parton, V.Z., 1976. Fracture mechanics of piezoelectric materials. Acta Astronautica 3, 671–683.

Shindo, Y., Narita, F., Tanaka, K., 1996. Electroelastic intensification near anti-plane shear crack in orthotropic piezoelectric ceramic strip. Theoretical and Applied Fracture Mechanics 25, 65–71.

Shindo, Y., Tanaka, K., Narita, F., 1997. Singular stress and electric fields of a piezoelectric ceramic strip with a finite crack under longitudinal shear. Acta Mechanica 120, 31–45.

Sosa, H., 1991. Plane problems in piezoelectric media with defects. International Journal of Solids and Structures 28, 491–505.

Sosa, H.A., Pak, Y.E., 1990. Three-dimensional eigenfunction analysis of a crack in a piezoelectric material. International Journal of Solids and Structures 26, 1–15.

Stroh, A.N., 1962. Steady state problems in anisotropic elasticity. Journal of Mathematical Physics 41, 77–103.

Suo, Z., Kuo, C.M., Barnett, D.M., Willis, J.R., 1992. Fracture mechanics for piezoelectric ceramics. Journal of the Mechanics and Physics of Solids 40, 739–765.

Theocaris, P.S., 1974. The order of singularity at a multi-wedge corner of a composite plate. International Journal of Engineering Science 12, 107–120.

Ting, T.C.T., 1986. Explicit solution and invariance of the singularities at an interface crack in anisotropic composites. International Journal of Solids and Structures 22, 965–983.

Tranter, C.J., 1948. The use of the Mellin transform in finding the stress distribution in an infinite wedge. Quarterly Journal of Mechanics and Applied Mathematics 1, 125–130.

Uchino, K., 1997. Piezoelectric Actuators and Ultrasonic Motors. Kluwer Academic Publishers, Norwell, MA.

Williams, M.L., 1952. Stress singularities resulting from various boundary conditions in angular corners of plates in extension. Journal of Applied Mechanics 19, 526–528.

Xu, X.L., Rajapakse, R.K.N.D., 2000. On singularities in composite piezoelectric wedges and junctions. International Journal of Solids and Structures 37, 3253–3275.